

CHAPTER 7

LIFE CYCLE COST ORIENTED SEISMIC DESIGN OPTIMIZATION: A MULTIOBJECTIVE APPROACH

Abstract: Life cycle cost is considered in this chapter for multiobjective design optimization of seismic steel moment resisting frame structures. Initial material/construction cost and lifetime seismic damage cost, which are usually added up in existing literature to form the total life cycle cost measure, act in the present study as separate objective functions, plus the number of different steel section types treated as the third objective function to roughly account for design complexity related additional construction expenses, which is important but difficult to be incorporated into the initial cost objective. The maximum interstory drift ratio is used as the single seismic performance index for a code-compliant design solution and is evaluated through a static pushover analysis. Effects of randomness and uncertainty in seismic demand and capacity estimates as well as in seismic hazards are considered in accordance with SAC/FEMA guidelines; as a result, the seismic damage cost is computed with confidence level dependent percentile limit state probabilities at prescribed drift ratio limits that demarcate a spectrum of performance levels with varied damage states. Compared to most of the existing life cycle cost design optimization procedures that usually use mean values of limit state probabilities and lead to a single design with a minimum (or sufficiently reduced) expected total life cycle cost, the present genetic algorithm based procedure integrates user-specified confidence level on damage cost estimate and produces a wide distribution of alternative designs that exhibits optimized tradeoff among selected conflicting objective functions. Therefore, designers have much freedom to select the final structural design with a preferred balance of initial cost and damage cost while taking into due account of the design complexity issue.

7.1 Introduction

Structural engineers tend to optimize the system they are designing based on different considerations such as cost-effectiveness, aesthetics, social/political issues, etc. In steel frame building designs, for example, widely used optimization objective functions include minimum structural weight, minimum compliance, a fully stressed state, desired component/system reliability levels, etc, many of which are related, either explicitly or implicitly, to present or future monetary expenses to some extent.

The consideration of both initial construction cost and lifetime cost (e.g., costs due to maintenance, operation, repair, damage, and/or failure consequences) leads to a so-called “life cycle cost” analysis under which the optimal design is the one that balances these two general cost items appropriately according to pre-selected criteria. It is, however, very difficult at the early design stage to quantitatively express various sources of initial cost with comparable accuracies. For example, estimation of material usage related expenses may be relatively easier. In contrast, it is a demanding task to quantify the precise relationship between the complexity of a proposed design and its associated labor/erection cost. Furthermore, future costs due to maintenance, inspection, as well as direct/indirect economic losses due to environmental attacks (wind, earthquake, etc.) are uncertain in nature and can only be evaluated in a probabilistic sense. As previous research examples, Wen and Shinozuka (1998) investigated cost-effective active structural control scenarios; Koh et al. (2000) evaluated cost-effectiveness for seismic-isolated bridges; Frangopol et al. (2001) performed life cycle cost analysis for optimal maintenance and inspection of bridge structural systems for reliable lifetime functionality.

The future cost considered in the study comes from monetary-equivalent losses due to seismic events during a structure’s lifetime; other future expenses (as well as possible benefits)

are not taken into account due to their usually independency to seismic structural resistance. The primary criterion of traditional code provisions is to ensure life safety and prevent structural collapse. Recent earthquakes, however, revealed that economic losses induced by less drastic structural damages as well as functional disruptions can also be enormous comparable to the structure's initial cost. Therefore, the concept of damage control needs to be considered appropriately in the design stage in order to reduce future economic losses. The idea of incorporating lifetime seismic damage cost into the structural design process can be traced back, for example, to Liu and Neghabat (1972) who proposed a cost optimization model for seismic structural design using a minimum life cycle cost criterion.

In the last decade, concepts of performance-based seismic design have been emerged and continuously developed as the new generation design methodologies. The most distinctive feature from conventional design practice is the explicit evaluation of actual structural performance under future seismic loading conditions expressed in probabilistic terms (e.g., ATC-40 1996; FEMA-273 1997; FEMA-350 2000). Permissible structural performances as well as damage states associated with each hazard level are both illustrated qualitatively based on previous earthquake-driven site inspections and are expressed quantitatively in terms of representative structural response indices (e.g., interstory drift ratio, axial column force). Structural designs conforming to these design guidelines with multiple limit states are expected not only to ensure life safety/collapse prevention under severe earthquakes but also to incur less damage-related direct/indirect consequences when subject to small to moderate seismic events.

By use of appropriate cost functions associated with varied damage states, designers have an opportunity to consider earthquake-related economic losses in a direct and explicit manner; seismic structural design based on life cycle cost analysis then becomes a tractable alternative. In

particular, the expected lifetime seismic damage cost could be derived by adding the product of each damage state cost and its associated expected failure probability during a lifetime.

Minimization of the expected life cycle cost, which is a direct sum of initial cost and the expected lifetime seismic damage cost, has primarily been the sole design criterion (i.e., objective function) that received fruitful research efforts. For example, Kang and Wen (2000) developed a design methodology based on the minimum expected life cycle cost and investigated its application in steel moment frame building design; using FEMA-released software HAZUS, Kohno and Collins (2000) investigated minimum life cycle cost design of reinforced concrete structures; Ang and Lee (2001) analyzed reinforced concrete buildings built in Mexico based on cost functions in terms of the Park-Ang damage index. It should be pointed out that these pioneering research efforts were based on a series of conventional trial designs with varied base shear levels around the codified values; no formal optimization algorithms were actually involved. Their conclusions were that the codified base shear level should be increased appropriately in order to minimize the expected total life cycle cost.

Theoretically speaking, the minimum life cycle cost criterion represents an ideal design philosophy of obtaining the most economical design from a risk-neutral perspective. In practice, however, this may not always hold due to the following reasons.

First, a single optimized design obtained from minimizing the expected life cycle cost does not take into account the fact that a risk-affine decision maker, who is willing to accept a higher risk of future seismic impacts, may prefer a code-compliant design with a lower initial cost (hence a lower structural capacity) and an associated higher damage cost, as compared to a risk-averse decision maker who would tend to do the opposite. Rather than passively accepting a single optimized design with no personal involvement, a structural engineer may be more

comfortable with selecting from a large design pool a particular structural design that meets his/her preferred resources allocation for initial expenses and damage reduction. Facing a preliminary design candidate, for example, a designer may expect an improved design solution that (1) has slightly increased initial investment while reducing the damage cost by a prescribed percentage or (2) has decreased initial cost while not altering damage cost significantly. Therefore, a viable approach is to treat initial cost and damage cost as two separate objective functions; the resulting distribution of tradeoff designs then allows the designer to select with freedom a design solution that balances these two general costs according to individual preference.

Second, accuracy levels associated with evaluation of different cost components may differ significantly. For the present investment, the initial material related construction cost may be relatively estimated with acceptable accuracy using well-documented cost handbooks such as Means (BCCD 1999); additional construction cost due to varied degree of design complexity, however, is more difficult to quantify and has not usually been considered explicitly in existing design optimization procedures. In construction of a steel frame building, for example, these additional costs include detailing cost and other labor-intensive construction operations, cost due to human errors such as misplacement of members, etc; the ease of construction will be very much dependent on the number of different member sizes and connection types being used, whether doublers and/or stiffeners are required, the number of column splices necessary, etc. Although attempts have been made to address this issue in the literature such as Carter (1999) who presented empirical equations to convert use of doublers and stiffeners into equivalent steel usage, there have been no consensus or widely accepted methods of relating design complexity to monetary values with comparable accuracy.

More importantly, quantification of seismic damage cost raises more accuracy concerns due to the following reasons: (1) there exist various sources of uncertainty/randomness in predicting structural capacity and seismic demands as well as in seismic excitations (FEMA 2000); sound treatment of these issues relies on appropriate probabilistic description and simplified models are necessary to yield a tractable engineering formulation; (2) assumptions inherent in developing a damage cost model and the subjective nature in defining discrete damage states as well as in the associated cost functions further lower the accuracy for damage cost objective evaluation.

Therefore, all relevant cost components in a life cycle cost analysis may not necessarily or meaningfully be addable unless they are of similar computational accuracies. It has been illustrated that determination of a single optimized design solution based on the direct-sum-of-costs approach may be sensitive to the actual relative proportioning of different cost components in the total life cycle cost (Kohn and Collins 2000). Wen et al. (2003) also stated that the minimum life cycle cost design is highly dependent on failure consequences. By treating different cost components as separate objective functions, designers may be able to make their own decision on the proportioning of different cost ingredients for the final compromise design, with knowledge of different accuracy associated with each cost component.

In response to the above concerns, a genetic algorithm (GA) based automated procedure is presented in this chapter for seismic design optimization of steel moment frame structures in accordance with 2000 NEHRP seismic provisions and AISC seismic steel design specifications. The life cycle cost is considered through two separate objective functions: initial cost and lifetime seismic damage cost. Degree of design complexity is roughly accounted for by the number of different steel section types as the third objective function, which provides an additional dimension to the resulting tradeoff optimized design solutions. The damage cost is

computed in this study with designer-specified confidence level related percentile limit state probabilities so that effects of randomness and uncertainty in seismic demand and capacity estimates as well as in seismic hazards are appropriately considered, following the SAC/FEMA guidelines (Cornell et al. 2002).

It should be noted that life cycle cost oriented design optimization with multiple objective functions have also been studied by other researchers. For example, Cheng et al. (1999) suggested a reliability-based optimization procedure for cost-effectiveness design and upgrading of seismic-resistant reinforced concrete building structures, using the target reliability and the minimum expected life cycle cost as two objective functions; GA was also selected as the primary search engine in conjunction with a fuzzy logic technique.

7.2 A multiobjective design optimization procedure

7.2.1 General formulation

The present multiobjective optimization problem can be conceptually stated as

Goal To obtain a distribution of optimized tradeoff seismic designs of steel moment frame structures with simultaneous minimization of three competing objective functions:

- (1) initial cost consisting of expenses due to construction of steel framework, metal deck, concrete, slabs, etc.;
- (2) degree of design complexity in terms of the number of different standard steel section types; and
- (3) lifetime seismic damage cost calculated with user-specified confidence level of limit state probabilities.

Subject to 2000 NEHRP seismic provisions;

AISC-LRFD steel design specifications; and

AISC seismic design provisions.

The above three objective functions strive for different design goals: minimization of initial cost seeks for an optimized design from the present economy viewpoint, while minimization of lifetime damage cost reduces the long-term risk due to loss of human life, injury and structural/nonstructural damage-related direct/indirect economic consequences during potential lifetime seismic events; the objective function of design complexity degree prevents the final design from being unnecessarily complicated in terms of number of different steel section types while balancing initial cost and damage cost. Only a simultaneous minimization of all these objective functions can satisfactorily lead to an overall economical design solution.

Figure 7.1 gives a flowchart of the present GA-based multiobjective optimization procedure integrated with a life cycle cost analysis. Following Kang and Wen (2000), the initial cost is based on unit prices of \$2,375/ton for steel beam/column members, \$1.86/ft² for metal decking, \$1.63/ft² for lightweight concrete slabs, and \$1.14/ft² and \$1.46/ft² for beam and column fireproofing, respectively. Evaluation of the lifetime seismic damage cost follows the methodology proposed by Kang and Wen (2000) and is presented in Section 7.2.2.

7.2.2 Calculation of lifetime seismic damage cost

Analytical Formula

Within a performance-based seismic design framework, the damage cost is related to attainment of different damage states defined by sound engineering experiences from previous earthquake investigations. Based on a Poisson process model of earthquake occurrences and an

assumption that damaged buildings are immediately retrofitted to their original intact conditions after each major damage-inducing seismic attack, Kang and Wen (2000) proposed the following formula for the expected damage cost with consideration of K damage states:

$$E[C_{seismic}(T, \mathbf{X})] = \frac{\nu}{\lambda} (1 - e^{-\lambda T}) \sum_{j=1}^K C_j P_j \quad (7.1)$$

where C_j = cost function of the j -th seismic damage state; P_j = mean value of the j -th damage state probability given seismic occurrence; ν = annual occurrence rate of significant earthquake events modeled by a Poisson process, and ν can be canceled in Equation 7.1 if the seismic damage cost associated with the first damage state, C_1 , is zero (Kang and Wen 2000); λ = annual monetary discount rate; T = service life of a new structure or remaining life of a retrofitted structure. Detailed derivation of Equation 7.1 is provided in Appendix C.

For the j -th damage state, the cost function is formulated as

$$C_j = C_j^{damage} + C_j^{content} + C_j^{relocation} + C_j^{economic} + C_j^{injury} + C_j^{fatality} \quad (7.2)$$

where C_j^{damage} = direct structural/nonstructural damage and repair cost; $C_j^{content}$ = cost due to loss of contents; $C_j^{relocation}$ = relocation cost; $C_j^{economic}$ = direct/indirect economic loss; C_j^{injury} = injury cost; $C_j^{fatality}$ = human fatality cost. Determination of these cost components can be found in Appendix D.

Definition of damage states

FEMA-273 associates performance levels of Immediate Occupancy (IO), Life Safety (LS), and Collapse Prevention (CP) performance levels with permissible interstory drift ratio limits of 0.7%, 2.5% and 5%, respectively (Table 7.1). Kang and Wen (2000) defined seven damage states

in terms of maximum interstory drift ratios to describe a spectrum of structural/nonstructural damage severity levels (Table 7.2), where the upper bound drift ratios for “light”, “heavy”, and “major” damage states were calibrated to the drift ratio limits corresponding to onsets of damage states that are worse than those associated with FEMA-273 IO, LS, and CP performance levels, respectively.

The deterministic drift ratio limits used in Kang and Wen are primarily for performance evaluation of pre-Northridge steel moment frames that typically experience connection fractures under severe seismic events (FEMA-273 1997), leading to less seismic capacities compared to post-Northridge steel SMRF designs that are equipped pre-qualified ductile connections and therefore exhibit improved seismic performances (Lee and Foutch 2000). Therefore, another set of drift ratio limits related more closely to the seven damage states defined in Table 7.2 is needed in the present study for design optimization of post-Northridge steel SMRF structures. In accordance with FEMA-350 (2000), median drift ratio capacities for IO and CP damage states (Tables 7.3 and 7.4) considering global structural behavior only are 2% and 10%, respectively. Because damage cost functions formulated in Kang and Wen are adopted in this study, other drift ratio limits that define the complete seven damage states are obtained by scaling drift ratio limits in Kang and Wen accordingly. Table 7.5 provides the present set of interstory drift ratio limits for the seven damage states. Note that the upper bound drift ratios of the “light” and “major” damage states are taken equal to median drift capacities of IO and CP performance levels in FEMA guidelines, respectively.

7.2.3 Treatment of randomness and uncertainty

Use of mean value of limit state probabilities

Aleatory and epistemic uncertainties are usually separately considered in probabilistic seismic performance evaluation of structures. Generally speaking, aleatory uncertainty refers to the record-to-record variability and the epistemic uncertainty is due to lack of sufficient knowledge in describing seismic events and structural performance. In accordance with Wen et al. (2003), Aleatory and epistemic uncertainties are referred to as “randomness” and “uncertainty”, respectively.

Mean estimates of limit state probabilities are usually used in the existing life cycle cost oriented design environment, which leads to the mean value of lifetime seismic damage cost estimate. To account for the randomness and uncertainty in the capacity and demand, for example, Wen and Foutch (1997) used an “uncertainty correction factor” that is defined as the ratio of the limit state probability with consideration of the model uncertainty to that in which the model uncertainty is ignored, i.e., a deterministic structural model is assumed. The limit state probability is multiplied by a correction factor:

$$C_F = 1 + \frac{1}{2} S^2 \beta_T^2 \quad (7.3)$$

where $\beta_T = \sqrt{\beta_{DR}^2 + \beta_{CR}^2 + \beta_{DU}^2 + \beta_{CU}^2}$ the coefficient of variation of the total randomness and uncertainty in the demand and capacity, with β_{DR}, β_{CR} = dispersion measure for randomness in drift demand and capacity, respectively and β_{DU}, β_{CU} = dispersion measure for uncertainty in drift demand and capacity, respectively; S = sensitivity coefficient to the change in structural capacity depending on the seismic hazard and the median structural capacity and can be obtained from

$$S = \frac{\ln R - \lambda_{LN}}{\zeta^2} \quad (7.4)$$

with R being the structural capacity in terms of median spectral acceleration, λ_{LN} and ζ two parameters of the assumed lognormal distribution for the seismic hazard in terms of median spectral accelerations at the fundamental natural period.

Alternatively, if the raw limit state probability is kept the same, median demand estimates considering the randomness in the seismic excitation only (assuming uncertainty in seismic hazard has been included) can be multiplied by another correction factor C_D :

$$C_D = 1 + \frac{1}{2} S \beta_T^2 \quad (7.5)$$

As another similar approach, the SAC/FEMA guidelines (Cornell et al. 2002) calculates the mean limit state probability as the following, assuming lognormal distributions for randomness/uncertainty in seismic hazard, demands, and capacity, respectively:

$$\bar{P} = \bar{H}(S_a^{\hat{C}}) \exp \left[\frac{1}{2} \frac{k^2}{b^2} \beta_T^2 \right] \quad (7.6)$$

where $\bar{H}(S_a^{\hat{C}})$ = mean estimate of spectral acceleration hazard associated with median drift capacity \hat{C} ; k = slope of the hazard curve, in log-log coordinates, at the hazard level of interest, i.e., the ratio of incremental change in S_{a,T_l} to incremental change in annual probability of exceedance, where S_{a,T_l} is the median 5%-damped elastic spectral response acceleration of the fundamental period T_l at a desired hazard level associated with the performance level; b = a coefficient relating the incremental change in demand to an incremental change in ground shaking intensity, at the hazard level of interest, typically taken as 1.0; β_T = the coefficient of

variation of the total randomness and uncertainty in the demand and capacity as defined in Equation 7.3.

Use of percentile value of limit state probabilities

Instead of using mean (i.e., expected) values of damage state probabilities to compute the damage cost with Equation 7.1, percentile values of limit state probabilities will be used in this chapter so that designer-specified confidence level can be appropriately incorporated in the life cycle cost oriented design process. The related approaches follow the SAC/FEMA guidelines (Cornell et al. 2002). Note that only the randomness/uncertainty parameters in seismic demand/capacity estimates as well as in seismic excitations that affect the calculation of P_j are considered herein; other parameters in Equation 7.1 are assumed deterministic. Under the present assumptions, the expectation is operated only on the random nature of number of seismic occurrence and their random occurrence times over the lifetime (Appendix C).

Two alternative approaches may be used in accordance with the SAC/FEMA guidelines. In the first approach, one multiplies the raw limit state probability, which is calculated with consideration of uncertainty/randomness in seismicity only, by a correction factor that accounts appropriately for uncertainty/randomness in both demand and capacity together with user-specified confidence level. The other approach keeps the raw limit state probability unchanged while modifying calculated drift demands (or capacity limits that define damage states) to reflect the effects of uncertainty/randomness. These two approaches are presented in detail as follows.

Approach I: modifying limit state probabilities

According to Cornell et al. (2002), the probability that *Demand* exceeds *Capacity*, P , at a given hazard level with a particular confidence level x can be evaluated as:

$$P^x = \hat{P} \exp[K_x \beta_p] \quad (7.7)$$

where $K_x = \Phi^{-1}(x)$ standardized normal variate associated with probability x of not being exceeded; \hat{P} the median estimate of P and β_p the dispersion measure for uncertainty in P , which are respectively calculated as

$$\hat{P} = \bar{H}(S_a^{\hat{c}}) \exp\left[\frac{1}{2} \frac{k^2}{b^2} (\beta_{DR}^2 + \beta_{CR}^2)\right] \quad (7.8)$$

$$\beta_p = \sqrt{\frac{k^2}{b^2} (\beta_{DU}^2 + \beta_{CU}^2)} \quad (7.9)$$

with the relevant variables defined as before. Derivation of these equations is briefly presented in Appendix E.

To implement this approach, one follows the steps as described below and schematically illustrated in Figure 7.2:

- (1) calculate the median drift demands at multiple pre-selected mean hazard levels;
- (2) a lognormal curve is fitted through these points relating to drift demand and hazard level pairs. This curve now represents the mean estimate of the hazard curve, from which one reads the exceedance probability associated with the median drift ratio capacities (2% and 10%) for IO and CP performance levels, respectively;

- (3) calculate the percentile exceedance probabilities associated with these two median drift capacities by multiplying a confidence level dependent correction factor that considers both randomness and uncertainty, according to the SAC/FEMA guidelines;
- (4) another lognormal curve is fitted through these two new data points. This curve is assumed to carry uniform confidence levels across all the limit state probabilities;
- (5) one reads from this new curve the limit state probabilities of the drift ratio limits that define each damage state; damage state probabilities given seismic occurrence are then evaluated using the equations as provided in Appendix C.

Approach II: modifying drift ratio demands/capacities

Alternatively, if the limit state probability is taken as mean estimate of the hazard curve at the selected hazard level (see Step 2 in Approach I), one may increase the calculated drift ratio demands or equivalently decrease the original drift ratio capacities so that effects of uncertainty/randomness in both demand and capacity are incorporated to meet user-defined confidence levels on estimation of limit state probabilities. The basic procedures in accordance with SAC/FEMA guidelines are discussed as below.

A confidence index parameter, λ_x , is first determined from the following factored-demand-to-capacity ratio:

$$\lambda_x = \frac{\gamma \gamma_a D}{\phi C} \quad (7.10)$$

where C = median structural capacity, such as interstory drift demand, obtained either by reference to default values in FEMA-350, or by rigorous direct evaluation; D = calculated seismic demand, obtained from a structural analysis; γ = a demand variability factor that

accounts for the variability inherent in the prediction of demand related to assumptions made in structural modeling and prediction of the character of ground shaking; γ_a = an analysis uncertainty factor that accounts for bias and uncertainty associated with the specific analytical procedure used to estimate structural demands as a function of ground shaking intensity; ϕ = a resistance factor that accounts for the uncertainty and variability inherent in the prediction of structural capacity as a function of ground shaking intensity.

The confidence level is then obtained through

$$\text{Confidence Level} = \Phi \left(\frac{1}{2} \cdot k \cdot \beta_{UT} - \frac{\ln \lambda_x}{b \beta_{UT}} \right) \quad (7.11)$$

where Φ = the standard Gaussian distribution operator; k = linear regression coefficient for hazard in logarithmic space, as defined in Equation 7.6; $\beta_{UT} = \sqrt{\beta_{DU}^2 + \beta_{CU}^2}$ an uncertainty measure equal to the vector sum of the logarithmic standard deviation of the variations in demand and capacity resulting from uncertainty; b = linear regression coefficient of drift demand on seismic intensity in logarithmic space, as defined in Equation 7.6. Derivation of these equations is also briefly discussed in Appendix E.

From Equation 7.10, one can obtain the confidence level x -dependent amplification factor for drift ratio demand as

$$\alpha_x = \frac{\gamma \gamma_a}{\phi \lambda_x} \quad (7.12)$$

At a specific hazard level, the calculated raw drift demand D is multiplied with α_x and then compared to the capacity C that defines a specific damage limit state (Table 7.5). It is expected

with a confidence level of x that demand does not exceed capacity under a given mean hazard level if the following inequality is satisfied:

$$\alpha_x D \leq C \quad (7.13)$$

Equivalently one may reduce the original drift capacity value of each of the seven performance levels and compare to the (non-amplified) drift demands. The demand does not exceed capacity with a confidence level of x under a given mean hazard level if the following inequality is met:

$$D \leq \frac{C}{\alpha_x} \quad (7.14)$$

These two equivalent approaches are schematically illustrated in Figures 7.3 and 7.4, respectively.

Implementation in this chapter

The approach of decreasing drift capacity limits while keeping both raw limit state probabilities and calculated drift demands unchanged is used in this chapter to account for effects of uncertainty/randomness in demand and capacity estimation. The damage states associated with IO and CP performance levels are used as the references for calibrating drift capacity values with user-defined confidence level on limit state probabilities.

Table 7.6 provides relevant default values for parameters used in Equations 7.10 and 7.11 that are excerpted from FEMA-350 for mid-rise (4-12 stories) steel SMRF structures, using the static pushover analysis as the primary analysis tool for estimating the maximum interstory drift demand. Note that parameters for other structural types and analysis procedures are also provided in FEMA-350. With these data, the confidence level for any given interstory drift

demand can be readily calculated; the resulting confidence level vs. maximum drift ratio demand curves for IO and CP performance levels are plotted in Figures 7.5 and 7.6, respectively.

As an inverse problem, drift ratio limits can then be determined such that, upper bound drift ratio limits (i.e., drift ratio capacity) that define IO and CP damage states can be read from these two curves at any user-defined confidence level. For illustration purposes, six confidence level values (40%, 50%, 60%, 70%, 80%, and 90%) are used to represent a wide range of confidence levels. For example, drift ratio limits associated with the 70% confidence level are 0.94% and 7.37% for IO and CP damage states, respectively, which are shown in Figures 7.5 and 7.6, respectively. A risk-averse designer may conservatively allow higher confidence levels for estimating limit state probabilities whereas a risk-affine designer would likely take lower confidence levels.

The remaining drift ratio limits that define the complete seven damage states are obtained by proportioning accordingly drift ratio limits of Kang and Wen (2000) in order to be consistent with the adoption of their damage cost functions in the present study. Denoted as *CL-40* through *CL-90* that indicate the respective confidence levels, the resulting complete six sets of drift ratio limits are listed in Table 7.7 where the upper bound drift ratios for “light” and “major” damage states are assumed consistent with drift ratios corresponding to, with varied confidence levels, onsets of damage states that are worse than FEMA-350 IO and CP damage states, respectively. The six sets of drift ratio limits are compared graphically to those provided in Kang and Wen (2000) in Figure 7.7.

Comments

Described as above, a lognormal curve is fitted through pairs of limit state probability vs. maximum drift ratio demand, from which the limit state probabilities corresponding to the drift ratio limits that define damage states are readily read. The lifetime seismic damage cost is then calculated using Equation 7.1. Although only the confidence level of the limit state probabilities associated with IO and CP damage states is explicitly considered in this study, it may reasonably assume that a uniform confidence level exists across all relevant limit state probabilities through the lognormal curve fitting. The resulting damage cost may then approximately bear a similar confidence level that is used to determine the respective set of drift ratio limits.

Generally speaking, if a higher confidence level is required to estimate limit state probabilities, the calculated occurrence probabilities of more severe damage states will increase, which indicates that more *calculated* damage cost would be anticipated than if a lower confidence level is assumed. It is clear that, for a given structural design, the calculated damage cost is in fact dependent upon the choice of confidence level for the exceedance probabilities of drift ratio limits that define relevant damage states.

Given a particular structural design, a risk-averse designer who associates a higher confidence level with limit state probabilities may possibly discard this design solution due to its high *calculated* damage cost; s/he may then look for another stronger design with reduced *calculated* damage cost while using the same set of drift ratio limits so that the confidence level is preserved. In contrast, a risk-affine designer may very likely accept the original design solution since s/he may think that the *calculated* damage cost (now with a lower confidence level on the limit state probabilities) is small enough; or s/he may even try to locate another weaker and thus more initial-cost competent code-compliant design solution if s/he judges that the

current design is unnecessarily too strong and would therefore be willing to accept additional *calculated* damage cost under the present lower confidence level on limit state probabilities.

A specific example design of the plane five-story four-bay plane moment frame is considered herein that consists of three different section types, W14X342 for all columns and W36X135 and W24X68 for beams at 1-3 and 4-5 floor levels, respectively, with an initial cost is \$1.284M. The calculated damage cost as sketched in Figure 7.8 turns out to be \$0.281M, \$0.319M, \$0.362M, \$0.415M, \$0.489M, and \$0.618M, respectively, for the six sets of drift ratio limits in Table 7.7. The “calculated damage cost” is briefly referred to as “damage cost” in the subsequent discussions.

In summary, significant features of the present use of confidence level dependent percentile limit state probability values based on SAC/FEMA guidelines are that: (1) effects of randomness and uncertainty in both seismic demand and capacity are fully incorporated; (2) drift ratio limits that demarcate different damage states can be specifically tailored for seismic design of post-Northridge new steel SMRF structures and for the performance evaluation procedure used (the static pushover analysis in this study); and (3) user-specified confidence level on limit state probability can be conveniently integrated into the determination of drift ratio limits and the resulting damage cost is then dependent upon designers’ risk-acceptance preference.

7.3 Numerical examples

The proposed GA based procedure is now applied to design optimization of the plane five-story four-bay steel SMRF structure described in Chapter 3. An annual discount rate of 5% and a service life of 50 years are assumed in Equation 7.1. Different sets of drift ratio limits defined in Table 7.7 are used, respectively, to calculate damage costs. The fundamental period is obtained from DRAIN-2DX and is used to determine the design base shear as well as to calculate nominal

design drift ratios, in accordance with 2000 NEHRP provisions. Relevant MATLAB programming is provided in Appendix F.

In the first example, initial cost and damage cost are lumped together to form the total life cycle cost, together with the number of different steel section types as two separate objective functions. This constitutes a direct extension of the existing research on design optimization based on life cycle cost minimization in that design complexity is now considered as an additional objective. In the second example, three separate objectives, namely, initial cost, number of section types, and damage cost are subject to simultaneous minimization, which represents a distinct departure from the existing life cycle cost oriented seismic design optimization by constructing a optimized tradeoff among all these three objective functions.

7.3.1 Minimum life cycle cost design considering degree of design complexity

Optimization results and tradeoff analysis

In this section, two separate objective functions are considered, i.e., the total life cycle cost and the number of different steel section types. Extension of research of Kang and Wen (2000) in the present study includes: (1) use of a formal optimization scheme (GA) to find the optimized design solutions, (2) explicit consideration of design complexity, and (3) incorporation of user-specified confidence level on limit state probabilities to compute the seismic damage cost.

With each of the six sets of drift ratio limits in Table 7.7, the proposed GA based optimization procedure is used to produce optimized design solutions. Figure 7.9 shows the generational evolution of the tradeoff curves for each set of drift ratio limits. It is observed that a large portion of evolution is achieved during the early stages up to the 50th generation. After the 100th generation, the improvement of the tradeoff curves is negligible. However, in order to

make a comparison with the second example where three objective functions are used that necessitates more generational computation, the present GA is terminated at the 200th generation for both numerical examples.

The optimized tradeoff design solutions obtained at the 200th generations are provided in Tables 7.8 through 7.13 for six sets of drift ratio limits, respectively. In each table, the optimized design for each particular section type number is the one that best possibly reduces the total life cycle cost among all frame designs with the same particular section type number. One observes that the design solutions provided in each table exhibit a strict tradeoff between the minimum total life cycle cost and the respective number of different section types, which are explicitly used in this example as two separate competing objective functions subject to simultaneous minimization. The globally minimum life cycle cost design is therefore inevitably equipped with the largest number of different section types, as shown in each table.

A careful study of the above tradeoff relationship reveals that, for optimized frame designs obtained with a given set of drift ratio limits, the minimum life cycle cost objective is very sensitive to the number of section types when such a number is small while it becomes insensitive when the section type number is relatively large. Take as an example the optimized designs obtained with the CL-70 set of drift ratio limits (Table 7.11). The life cycle cost associated with the design of two section types is \$1.897M. By simply introducing one, two, and three net new section types, the life cycle cost is reduced by 7.5%, 10.7%, and 13.2%, respectively. Use of even more section types does not significantly help to save economy in terms of the life cycle cost: compared to the design with two different section types, designs with six and nine section types have a reduction in the life cycle cost of only 14.9% and 16.0%, respectively. The additional construction cost due to the increased design complexity in terms of

different section type numbers for the latter designs, however, may well overshadow possible savings in the life cycle cost.

The practical implication is that seeking for a minimum life cycle cost design should be balanced with reasonable degree of design complexity (in terms of number of different section types herein) in order to strive for an overall lifetime economical design. It is reiterated that existing steel design optimization procedures based on the minimum life cycle cost criterion do not explicitly consider design complexity issues and, as a result, they may very likely lead to a final structural design with unnecessarily many different section types; if subjectively restraining the number of section types used in the structure, one may not always obtain a truly economical design solution without an explicit analysis of tradeoff expanding over all possible numbers of section types.

Also listed in Tables 7.8 through 7.13 are the associated nominal design drift ratios obtained with the codified elastic analysis procedure per 2000 NEHRP provisions as well as the actual system yield level resulting from the static pushover analysis. As discussed in Chapter 5, optimized design solutions with a (near) active design drift ratio constraint are usually close to the minimal weight (or minimal initial cost) design, which, from a life cycle cost point of view, may not be a preferred design solution due to lack of explicit control of damage cost through consideration of a spectrum of damage states. Seismic designs based on an appropriately selected more stringent design drift ratio limit may perform more satisfactorily in that initial cost and damage cost are balanced to achieve a minimized life cycle cost objective. The minimum life cycle cost designs with varied numbers of different section types, which are obtained with the CL-70 set of drift ratio limits, for example, have a reduced design drift ratio of $(1.39 \pm 0.05)\%$, as compared to 2.0% specified in 2000 NEHRP for the present steel SMRF design.

Effects of confidence levels on minimum life cycle cost designs

Unlike most of the existing life cycle cost oriented seismic design procedures where mean-valued limit state probabilities are used for damage cost calculation, the present study considers user-specified confidence levels on limit state probabilities (through different sets of drift ratio limits). The effects of confidence levels on the minimum life cycle cost designs are investigated herein. Tables 7.14 to 7.16 provide, for each confidence level dependent set of drift ratio limits, minimum life cycle cost designs of the same small (2), medium (5), and largest number of different section types, respectively.

Table 7.14 provides minimum life cycle cost designs with two different section types. It is seen that the identical design solution is obtained for CL-40 to CL-70 sets of drift ratio limits. For CL-80 and CL-90 sets of drift ratio limits, a new design with a 5.4% increase in initial cost is found instead; the system yield coefficient increases from 0.350 to 0.394 accordingly. Minimum life cycle cost designs with five different section types are listed in Table 7.15. As the confidence level increases from 40% to 70% and 90%, the system yield coefficient increases from 0.326 to 0.374 and 0.377, respectively, and initial cost increases from \$1.259M to \$1.295M and \$1.297M, respectively. Similar trends are also observed in Table 7.16 for designs with overall minimum life cycle cost for each set of drift ratio limits.

In summary, the general observation is that, for minimum life cycle cost designs with similar degree of design complexity, higher structural lateral force resistance is generally required as confidence level on limit state probabilities increases. This can be explained as follows: the higher the confidence level on limit state probabilities is assumed, the larger the damage cost is calculated; therefore, a stronger design solution is warranted to optimally balance the calculated damage cost in order to achieve the minimum life cycle cost objective.

Percentage differences in initial costs of the two particular designs obtained using CL-40 and CL-90 in Tables 7.14 to 7.16 are only 5.4%, 3.0%, and 6.2%, respectively. For the structural resistance capacity in terms of system yield coefficient, the percentage differences are 12.6%, 15.6%, and 19.0%, respectively. The general conclusion is that dependence of steel designs (especially in terms of the initial cost) on the confidence level is not significant when the minimum life cycle cost criterion is used for design optimization.

Performance evaluation of globally minimum life cycle cost designs

Optimized frame designs with globally minimum life cycle cost using each set of drift ratio limits as provided in Table 7.16 are subject to detailed performance evaluations. Nominal drift ratio profiles of these designs are plotted in Figure 7.10; normalized static pushover curves are presented in Figure 7.11. It is again observed that confidence level does not have significant effects on these overall minimum life cycle cost designs in terms of either initial cost (Figure 7.12) or actual system yield level (Figure 7.13).

Nonlinear time history analyses are then performed to obtain the most accurate estimates of seismic demands on these frame designs. Sets of twenty SAC ground motion records representing seismic hazard levels with exceedance probabilities of 50% and 2% in 50 years for Los Angeles area with soil type D (as described in Chapter 3) are used. Figure 7.14 plots the median (50th percentile), 84th percentile, and 95th percentile values of peak interstory drift ratio demand profiles for each design at the above two hazard levels, respectively; the maximum peak drift demands are excerpted and plotted in Figure 7.15. Fitted by a lognormal distribution of the median maximum interstory drift ratio demands computed by time history analysis vs. respective hazard level exceedance probabilities, seismic performance curves for these representative designs are plotted in Figure 7.16 using 50-year exceedance probabilities

and in Figure 7.17 using annual exceedance probabilities. Their seismic performances are very similar to one another.

7.3.2 Design optimization with three objective functions

In Section 7.3.1, a minimum life cycle cost criterion has been used in the design optimization. As discussed in Section 7.1, a designer may want to actively select, with self-specified confidence level on limit state probabilities, a structural design solution based on his/her own preferred balance between initial cost and damage cost other than the balance implied by the life cycle cost minimization.

In response to these considerations, the initial cost and damage cost are treated in this section as two separate objective functions, together with the number of different section types as the third objective function. The GA-based optimization procedure is now performed using each of the six sets of confidence level dependent drift ratio limits (Table 7.7) and the algorithm run is terminated at the 200th generation, which is the same as in Section 7.3.1. The optimization results are analyzed as follows.

Tradeoff among three objective functions

The optimized design solutions obtained by use of the CL-70 set of drift ratio limits are analyzed herein for illustration purposes. A total of 398 optimized design solutions are obtained the 200th generation. As shown in Figure 7.18, all these 398 designs form a curved surface in the space spanned by the present three objective functions and constitute the best possible tradeoff among them. These optimized designs are then projected onto a plane formed by the initial cost and damage cost axes, as plotted in Figure 7.19. A tradeoff trend can be clearly identified although designs with various numbers of different section types are mixed.

Note that the design with the traditional minimum life cycle cost is simply a single point in these figures. Facing this large pool of alternative designs, a designer now has much flexibility to select the final design solution that balances initial cost and damage cost in the most preferred manner with allowable number of different section types.

In order to have a better view of the tradeoff trend among costs without interference with the number of section types objective function, damage cost vs. initial cost with each particular number of section types is plotted in Figure 7.20. A rigorous 2D tradeoff curve is now observed for each specific section type number because initial cost and damage cost are used as two independent competing objective functions in the present optimization problem. As a general rule, the larger the number of section types is, the closer a design solution is to either cost axis due to more flexibility in selecting section types for reduction of either cost objective function. It is also noticed that tradeoff curves for smaller numbers of section types are usually more ‘continuous’ than those associated with larger numbers of section types. This is largely because the GA based optimization procedure has not adequately explored design spaces with larger section type numbers up to the 200th generation. For example, there are only two optimized designs with ten different section types. More optimized design solutions would be expected as the generational evolution process continues.

Figure 7.21 plots initial cost, damage cost, and sum of initial and damage costs (i.e., total life cycle cost) against the system yield coefficient S_y , respectively, for all 398 optimized designs. It is observed that S_y is very much positively correlated to the initial cost and therefore it also establishes an approximate tradeoff against the damage cost objective function. The approximation in tradeoff exists because S_y is not directly used as an objective function in the optimization process. The nominal design yield level in accordance with NEHRP provisions is

about 0.11. The plot of life cycle cost vs. S_y indicates that, by use of the CL-70 set of drift ratio limits, the optimized system yield level associated with minimum life cycle cost is about 2 to 2.5 times higher than the nominal value. Figure 7.22 further illustrates the monetary costs - S_y relationship for each number of section types, respectively.

From another viewpoint, Figure 7.23 plots initial cost, damage cost, and life cycle cost against the nominal design drift ratio, respectively, for all 398 optimized designs with varied numbers of section types. Apparently the design drift ratio is negatively correlated with the initial cost because a design solution with larger initial cost will typically have larger resistance and hence less drift demands. A design with larger drift demands indicates a lower resistance and thus leads to larger seismic damage cost, as shown in the second plot in Figure 7.23 where the design drift ratio is positively correlated to the damage cost. The plot of life cycle cost vs. design drift ratio shows that the optimized nominal drift ratio associated with a minimized life cycle cost is approximately 1.4%; in contrast, the allowable nominal drift ratio is 2% for the present steel SMRF structure per 2000 NEHRP.

The implication is that a code-compliant solution controlled by the allowable drift limit, which is a common seismic design practice, might not be the most desirable solution from a life cycle cost optimization viewpoint due to the associated enormous lifetime damage cost. Figure 7.24 further illustrates monetary costs vs. design drift ratio relationships for each number of section types. Because the design drift ratio is not used as a primary objective function in the present optimization, it may not necessarily constitute rigorously monotonic relationship with these initial cost or damage cost objective function.

The significance of formulating the life cycle cost design problem as a multiobjective optimization is that the optimized tradeoff relationship of initial cost, damage cost, and other

relevant objective functions can be explicitly obtained, based on which a designer has an opportunity to balance different cost components in an active and preferred fashion that reflects personal risk-acceptance levels. As a comparison, the minimum life cycle cost criterion may be viewed as a special as well as passive balance effort.

Minimum life cycle cost designs with varied degrees of design complexity

The minimum life cycle cost design for each number of different section types is identified from the 398 optimized designs at the 200th generation obtained using the CL-70 set of drift ratio limits. Unlike minimum life cycle cost designs that are directly obtained from an optimization process in Section 7.3.1, here design solutions of minimum life cycle cost are found indirectly as by-products out of the optimization with initial cost and damage cost as two separate objective functions. As a result, a rigorous tradeoff between the total life cycle cost and the number of different section types may not necessarily be guaranteed.

Table 7.20 provides detailed information for such minimum life cycle cost design solutions, which are compared to minimum life cycle cost designs obtained in the Section 7.3.1 in Figure 7.25 and are sketched in Figure 7.26 with line thickness proportional to section modulus. Note that the design with ten section types is discarded due to inadequate exploration for such case up to the 200th generation. From Table 7.20, it is seen that the associated optimized nominal design drift ratios are in the range of 1.3% and 1.5%, the actual system yield coefficients S_y are averaged as 0.34, which are also approximately observed in Figures 7.21 to 7.24.

The general tradeoff between the minimum life cycle cost and the associated number of section types still exists except for larger section type numbers for which the optimization search is inadequate up to the present 200th generation. Similar to observations in Section 7.3.1, the life cycle cost is much more sensitive to the number of section types when such a number is small.

For example, the minimum life cycle cost for the design with two section types is \$1.897M while the minimum life cycle cost is reduced by 10.4% to \$1.699M by simply introducing another new section type. The life cycle cost reduction rate becomes very slow when the number of section types is higher than five. For example, the minimum life cycle cost for the design with five section types is \$1.643M while the globally minimum life cycle cost at the 200th generation is \$1.617M that is associated with the design with eight different section types, indicating 1.6% difference only. The increased construction cost may negate such unnecessarily complex designs in order to achieve an overall cost-competent design solution.

Effects of confidence levels on minimum life cycle cost designs

The optimized designs in the above discussions are obtained using the set of drift ratio limits corresponding to a 70% confidence level on the limit state probabilities associated with various damage states (especially at IO and CP). Another designer may select other confidence levels based on his/her own experience and/or preference, provided the design solution conforms to relevant seismic design provisions. Effects of confidence levels on the outcomes of life cycle cost oriented design optimization are investigated herein using all six sets of drift ratio limits, respectively.

For each set of drift ratio limits, the minimum life cycle cost design for each number of different section types is identified and is reported in Tables 7.17 to 7.22, respectively. Figure 7.25 compares graphically minimum life cycle cost design solutions obtained from both direct and indirect life cycle cost optimization processes. It is observed that both optimization approaches in general produce similar optimized design solutions in terms of minimum life cycle cost with each set of drift ratio limits. In particular, it seems that the indirect approach

provides better results for designs with smaller number of section types while the direct approach excels for designs with larger number of section types.

Minimized initial cost design with damage cost constraint

Another design situation is considered herein where a designer wants to constrain the calculated damage cost to, for example, \$0.3M while minimizing the initial cost. For illustration purposes only, suppose five different section types are to be used. As discussed previously, the damage cost calculated with different confidence levels (in terms of varied sets of drift ratio limits) may differ significantly for a given design solution; likewise, design solutions with distinct structural capacities will be obtained in order to incur similar calculated damage costs with different confidence levels.

Table 7.23 provides six designs that conform to the above selection rules. These designs are also sketched in Figure 7.27, with line thickness proportional to section modulus. For drift ratio limit sets corresponding to confidence levels of 40% to 90%, the actual system yield coefficient varies from 0.325 to 0.556 while the initial cost increases accordingly from \$1.209M to \$1.754M, respectively. Figures 7.28 and 7.29 plot height-wise nominal design drift ratio profiles and static pushover curves for these alternative designs, respectively. Effects of confidence level on these structural designs are plotted in terms of initial cost (Figure 7.30) and actual system yield level (Figure 7.31).

A confidence level on limit state probabilities is usually specified by designers before a life cycle cost oriented design optimization is launched. The higher the confidence level is, the more conservative the designer becomes for evaluating the damage cost. A risk-affine designer may readily accept the design obtained using the set of drift ratio limits associated with, for example, a 40% confidence level and an initial cost of \$1.209M is spent. In contrast, a risk-

averse designer would be willing to accept more initial investment so that the resulting stronger structural design incurs the similar calculated damage cost but with a much higher confidence level. For instance, the design solution with CL-80 set of drift ratio limits requires an initial cost of \$1.552M, which indicates a 28.4% increase from that of the design solution with CL-40 set of drift ratio limits.

When facing a subset of frame design candidates preliminarily selected from a distribution of optimized tradeoff alternative designs, a designer takes the responsibility to determine the final design solution based on sound engineering experience and/or personal preference. Detailed structural performances may be evaluated to facilitate the judgment. Figure 7.32 plots the median, 84th percentile, and 95th percentile peak interstory drift ratio demand profiles, which are obtained from nonlinear dynamic analyses, for these six designs at 50/50 and 2/50 hazard levels, respectively; the maximum peak drift demands are excerpted and plotted in Figure 7.33. The results are in general agreement with those obtained from the static pushover analysis in that designs obtained with higher confidence levels usually have less drift demands. Seismic performance curves for these alternative designs are plotted in Figures 7.34 using 50-year exceedance probabilities and in Figures 7.35 using annual exceedance probabilities. Again, these designs demonstrate varied seismic resistances.

7.4 Summary

This chapter presented an automated design optimization procedure for seismic design of steel moment frame structures based on life cycle cost considerations. Three objective functions were used: initial cost, lifetime seismic damage cost, and number of different steel section types that approximately accounts for degree of design complexity. Each design solution complied with 2000 NEHRP seismic provisions and AISC-LRFD seismic steel design specifications.

Compared to most of the life cycle cost oriented design procedures existing in the literature, distinct features of the present research are:

- (1) Unlike existing life cycle cost oriented procedures that are based on a series of conventional trial designs, the present procedure utilizes a genetic algorithm as the search engine for the posed multiobjective optimization problem, which leads to design solutions with truly optimized objective measures. It has shown that, a code-compliant structural design controlled by the allowable nominal design drift limit, which is a common seismic design practice, might not be the most desirable solution from a life cycle cost optimization viewpoint due to the associated enormous damage cost. Optimized nominal drift ratio limits and actual system yield levels are qualitatively identified for structural designs that minimize the life cycle costs.
- (2) Design complexity issues are not (explicitly) considered in most of the existing life cycle cost oriented design procedures and, as a result, the additional construction cost of an unnecessarily complex design solution has not been appropriately accounted for in estimating initial expenses. In the present study, degree of design complexity is explicitly albeit approximately considered through the number of different standard steel section types as a separate objective function. This new formulation helps designers to find a cost-competent structural design with reasonable design complexity.
- (3) Most of the existing procedures use a minimum life cycle cost criterion. In the present study, the life cycle cost is considered by two separate objective functions, i.e., initial cost and lifetime seismic damage cost, together with the number of different standard steel section types. This multiobjective formulation produces a wide distribution of design solutions that exhibit the best possible tradeoff with respect to these three

objectives. The significant advantage is that a designer can select a final design solution that balances different cost aspects according to personal experience/preference and not necessarily the design solution bearing the minimum life cycle cost. In addition, numerical examples have shown that, for designs with smaller numbers of different section types, the total life cycle cost may be more reduced via GA by treating initial cost and damage cost as separate objective functions due to the presence of more optimized tradeoff designs in the optimization process, as compared to design optimization with total life cycle cost as the only cost objective.

- (4) Mean values of limit state probabilities are usually used in the exiting literature to quantify the expected seismic damage cost. In accordance with SAC/FEMA guidelines of considering uncertainty/randomness in both seismic demands and capacity, limit state probabilities in this study are quantified in terms of percentile values with user-specified confidence level, based on which the damage cost is calculated. This treatment provides an opportunity to integrate designers' risk-acceptance level into the life cycle cost design optimization process. Numerical examples illustrated that, for a risk-averse designer who demands higher confidence levels on limit state probabilities and hence on the damage cost calculation, a structural design with larger lateral resistance capacity is usually warranted; in contrast, a weaker code-complaint design solution may be accepted by risk-affine designers who prefer a lower confidence level instead.

As a word of caution, one should be aware of the approximate nature of the equivalent SDOF that represents the original MDOF system through a static pushover analysis, which might prefer certain member sizing patterns to others. Therefore it is best used for the preliminary design stage. A more accurate nonlinear time history response analysis is always helpful in the final

decision-making stage to verify actual seismic performance of a design solution obtained using the approximate approach. The computational expenses prohibit the direct use of time history analysis in the present GA based optimization procedure. Nevertheless, the procedure presented herein is viable to determine how structural materials should be distributed when life cycle costs are reasonably considered. The large pool of optimized code-conforming alternative designs leaves a designer much freedom to select the one that best compromises his/her goals represented by relevant objective functions.

Table 7.1 Structural performance levels (FEMA-273 1997)

	Immediate Occupancy	Life Safety	Collapse Prevention
Primary system	Minor local yielding at a few places. No fractures. Minor buckling or observable permanent distortion of members	Hinges form. Local buckling	Extensive distortion of beams and column panels. Many fractures at moment connections, but shear connections remain intact
Secondary system	Same as primary	Extensive distortion of beams and column panels. Many fractures at moment connections, but shear connection remain intact	Same as primary
Interstory drift	0.7% transient; negligible permanent	2.5% transient; 1% permanent	5% transient or permanent

Table 7.2 Damage state-related performance levels (Kang and Wen 2000)

Performance level	Damage state	Drift ratio (%)	Description (FEMA-227 1992)
I	None	$\Delta < 0.2$	No damage
II	Slight	$0.2 < \Delta < 0.5$	Limited localized minor damage not requiring repairs
III	Light	$0.5 < \Delta < 0.7$	Significant localized damage of some components generally not requiring repairs
IV	Moderate	$0.7 < \Delta < 1.5$	Significant localized damage of many components warranting repairs
V	Heavy	$1.5 < \Delta < 2.5$	Extensive damage requiring major repairs
VI	Major	$2.5 < \Delta < 5.0$	Major widespread damage that may result in the facility being razed, demolished, or repaired
VII	Destroyed	$\Delta > 5.0$	Total destruction of the majority of the facility

Table 7.3 Descriptive building performance levels (FEMA-350 2000)

	Immediate Occupancy	Collapse Prevention
Overall damage	Light	Severe
General	Structure substantially retains original strength and stiffness. Minor cracking of facades, partitions, ceilings, and structural elements. Elevators can be restarted. Fire protection operable.	Little residual stiffness and strength, but gravity loads are supported. Large performance drifts. Some exists may be blocked. Exterior cladding may be extensively damaged and some local failures may occur. Building is near collapse.
Nonstructural	Equipment and contents are generally secure, but may not operate due to mechanical failure or lack of utilities.	Extensively damage.

Table 7.4 Structural performance levels (FEMA-350 2000)

Elements	Immediate Occupancy	Collapse Prevention
Girder	Minor local yielding and buckling at a few places	Extensive distortion; local yielding and buckling. A few girders may experience partial fractures
Column	No observable damage or distortion	Moderate distortion; some columns experience yielding. Some local buckling of flanges
Beam-column connection	Less than 10% of connections fractured on any one floor, minor yielding at other connections	Many fractures with some connections experiencing near total loss of capacity
Panel zone	Minor distortion	Extensive distortion
Column splice	No yielding	No fractures
Base plate	No observable damage or distortion	Extensive yielding of anchor bolts and base plate
Interstory drift	Less than 1% permanent	Large permanent

Table 7.5 The present drift ratio limits of seven damage states

Performance level	Damage state	Drift ratio (%)
I	None	$\Delta < 0.5$
II	Slight	$0.5 \leq \Delta < 1.5$
III	Light	$1.5 \leq \Delta < 2.0$
IV	Moderate	$2.0 \leq \Delta < 3.5$
V	Heavy	$3.5 \leq \Delta < 5.5$
VI	Major	$5.5 \leq \Delta < 10.0$
VII	Destroyed	$\Delta > 10.0$

Table 7.6 Confidence level calculation parameters for mid-rise steel SMRF by static pushover analysis with global interstory drift ratios as the performance index (FEMA-350)

Performance level	Demand variability factor γ	Analysis uncertainty factor γ_a	Capacity C (%)	Resistance factor ϕ	Uncertainty coefficient β_{UT}
IO	1.4	1.45	2	1.0	0.2
CP	1.2	0.99	10	0.85	0.4

Table 7.7 Sets of drift ratio limits associated with varied confidence levels for limit state probabilities

Drift Ratio [%] Confidence Level Damage Limit State	CL-40	CL-50	CL-60	CL-70	CL-80	CL-90
None	$\Delta < 0.31$	$\Delta < 0.30$	$\Delta < 0.28$	$\Delta < 0.27$	$\Delta < 0.25$	$\Delta < 0.23$
Slight	$0.31 \leq \Delta < 0.79$	$0.30 \leq \Delta < 0.75$	$0.28 \leq \Delta < 0.71$	$0.27 \leq \Delta < 0.67$	$0.25 \leq \Delta < 0.63$	$0.23 \leq \Delta < 0.58$
Light	$0.79 \leq \Delta < 1.10$	$0.75 \leq \Delta < 1.05$	$0.71 \leq \Delta < 0.99$	$0.67 \leq \Delta < 0.94$	$0.63 \leq \Delta < 0.88$	$0.58 \leq \Delta < 0.81$
Moderate	$1.10 \leq \Delta < 2.77$	$1.05 \leq \Delta < 2.54$	$0.99 \leq \Delta < 2.34$	$0.94 \leq \Delta < 2.14$	$0.88 \leq \Delta < 1.93$	$0.81 \leq \Delta < 1.67$
Heavy	$2.77 \leq \Delta < 4.85$	$2.54 \leq \Delta < 4.42$	$2.34 \leq \Delta < 4.02$	$2.14 \leq \Delta < 3.63$	$1.93 \leq \Delta < 3.23$	$1.67 \leq \Delta < 2.75$
Major	$4.85 \leq \Delta < 10.06$	$4.42 \leq \Delta < 9.10$	$4.02 \leq \Delta < 8.22$	$3.63 \leq \Delta < 7.37$	$3.23 \leq \Delta < 6.50$	$2.75 \leq \Delta < 5.45$
Destroyed	$\Delta \geq 10.06$	$\Delta \geq 9.10$	$\Delta \geq 8.22$	$\Delta \geq 7.37$	$\Delta \geq 6.50$	$\Delta \geq 5.45$

Table 7.8 Minimum life cycle cost designs of varied section type numbers with CL-40 set of drift ratio limits and use of sum of initial cost and damage cost as one objective function

# of Section Types	2	3	4	5	6	7	8
Section Group ID	C1	W14X342	W14X342	W14X370	W14X370	W14X233	W14X233
	C2	W14X342	W14X342	W14X370	W14X370	W14X370	W14X370
	C3	W14X342	W14X342	W14X370	W14X370	W14X370	W14X370
	C4	W14X342	W14X342	W14X176	W14X176	W14X176	W14X145
	C5	W14X342	W14X342	W14X370	W14X370	W14X370	W14X370
	C6	W14X342	W14X342	W14X370	W14X370	W14X370	W14X370
	B1	W36X135	W36X135	W36X135	W36X135	W36X135	W36X135
	B2	W36X135	W36X135	W36X135	W36X135	W36X135	W36X135
	B3	W36X135	W36X135	W36X135	W36X135	W36X135	W33X118
	B4	W36X135	W21X62	W27X84	W27X84	W27X84	W27X94
	B5	W36X135	W36X135	W27X84	W21X50	W18X50	W18X46
Design Drift Ratio [%]	1.44	1.45	1.33	1.43	1.48	1.51	1.48
System Yield Coeff.	0.350	0.326	0.342	0.326	0.326	0.308	0.310
System Overstrength	3.51	3.41	3.47	3.35	3.45	3.31	3.33
Initial Cost [\$M]	1.343	1.311	1.274	1.259	1.226	1.211	1.201
Damage Cost [\$M]	0.377	0.303	0.290	0.253	0.275	0.267	0.274
Total LCC [\$M]	1.721	1.614	1.563	1.511	1.501	1.477	1.475

Table 7.9 Minimum life cycle cost designs of varied section type numbers with CL-50 set of drift ratio limits and use of sum of initial cost and damage cost as one objective function

# of Section Types	2	3	4	5	6	7	8	9
Section Group ID	C1	W14X342	W14X342	W14X342	W14X342	W14X257	W14X257	W14X233
	C2	W14X342	W14X342	W14X342	W14X342	W14X342	W14X342	W14X342
	C3	W14X342	W14X342	W14X342	W14X342	W14X342	W14X342	W14X370
	C4	W14X342	W14X342	W14X342	W14X176	W14X176	W14X176	W14X176
	C5	W14X342	W14X342	W14X342	W14X342	W14X342	W14X311	W14X311
	C6	W14X342	W14X342	W14X342	W14X342	W14X342	W14X311	W14X311
	B1	W36X135	W36X135	W36X135	W36X135	W36X135	W36X135	W36X135
	B2	W36X135	W36X135	W36X135	W36X135	W36X135	W36X135	W36X135
	B3	W36X135	W36X135	W36X135	W36X135	W36X135	W33X118	W33X130
	B4	W36X135	W24X55	W27X84	W24X94	W24X76	W27X84	W27X84
	B5	W36X135	W36X135	W21X50	W21X50	W21X57	W21X50	W21X50
Design Drift Ratio [%]	1.44	1.45	1.39	1.47	1.46	1.43	1.43	1.43
System Yield Coeff.	0.350	0.325	0.324	0.331	0.321	0.305	0.319	0.319
System Overstrength	3.51	3.40	3.38	3.49	3.47	3.31	3.46	3.46
Initial Cost [\$M]	1.343	1.308	1.283	1.232	1.207	1.200	1.190	1.188
Damage Cost [\$M]	0.427	0.342	0.306	0.304	0.313	0.312	0.310	0.309
Total LCC [\$M]	1.770	1.650	1.589	1.535	1.520	1.512	1.500	1.496

Table 7.10 Minimum life cycle cost designs of varied section type numbers with CL-60 set of drift ratio limits and use of sum of initial cost and damage cost as one objective function

# of Section Types	2	3	4	5	6	7	8	
Section Group ID	C1	W14X342	W14X370	W14X370	W14X370	W14X370	W14X233	W14X257
	C2	W14X342	W14X370	W14X370	W14X370	W14X370	W14X370	W14X370
	C3	W14X342	W14X370	W14X370	W14X370	W14X370	W14X370	W14X398
	C4	W14X342	W14X370	W14X176	W14X176	W14X176	W14X176	W14X176
	C5	W14X342	W14X370	W14X370	W14X370	W14X370	W14X370	W14X370
	C6	W14X342	W14X370	W14X370	W14X370	W14X370	W14X370	W14X370
	B1	W36X135	W36X135	W36X135	W36X135	W36X150	W36X150	W36X150
	B2	W36X135	W36X135	W36X135	W36X135	W36X150	W36X150	W36X150
	B3	W36X135	W36X135	W36X135	W36X135	W36X135	W33X130	W33X130
	B4	W36X135	W27X84	W27X84	W27X84	W30X99	W30X99	W30X99
	B5	W36X135	W27X84	W27X84	W21X50	W21X44	W18X46	W21X44
Design Drift Ratio [%]	1.44	1.37	1.33	1.43	1.42	1.43	1.40	
System Yield Coeff.	0.350	0.344	0.342	0.326	0.359	0.349	0.349	
System Overstrength	3.51	3.46	3.47	3.35	3.57	3.61	3.56	
Initial Cost [\$M]	1.343	1.338	1.274	1.259	1.275	1.241	1.249	
Damage Cost [\$M]	0.483	0.387	0.371	0.325	0.295	0.310	0.301	
Total LCC [\$M]	1.827	1.725	1.645	1.584	1.570	1.551	1.550	

Table 7.11 Minimum life cycle cost designs of varied section type numbers with CL-70 set of drift ratio limits and use of sum of initial cost and damage cost as one objective function

# of Section Types	2	3	4	5	6	7	8	9	
Section Group ID	C1	W14X342	W14X370	W14X370	W14X370	W14X370	W14X233	W14X257	W14X233
	C2	W14X342	W14X370	W14X370	W14X370	W14X370	W14X370	W14X398	W14X426
	C3	W14X342	W14X370	W14X370	W14X370	W14X370	W14X370	W14X398	W14X398
	C4	W14X342	W14X370	W14X370	W14X211	W14X176	W14X176	W14X176	W14X176
	C5	W14X342	W14X370	W14X370	W14X370	W14X370	W14X370	W14X370	W14X370
	C6	W14X342	W14X370	W14X370	W14X370	W14X370	W14X370	W14X370	W14X370
	B1	W36X135	W36X150	W36X150	W36X150	W36X150	W36X150	W36X150	W36X150
	B2	W36X135	W36X150	W36X150	W36X150	W36X150	W36X150	W36X150	W36X150
	B3	W36X135	W36X150	W36X150	W36X150	W36X135	W33X130	W36X135	W63X135
	B4	W36X135	W27X84	W27X84	W24X94	W30X99	W30X99	W30X99	W30X99
	B5	W36X135	W27X84	W24X55	W24X55	W21X44	W16X50	W21X44	W21X44
Design Drift Ratio [%]	1.44	1.31	1.30	1.35	1.42	1.43	1.41	1.42	
System Yield Coeff.	0.350	0.378	0.365	0.374	0.359	0.349	0.358	0.358	
System Overstrength	3.51	3.68	3.59	3.70	3.57	3.61	3.59	3.59	
Initial Cost [\$M]	1.343	1.357	1.344	1.295	1.275	1.243	1.259	1.259	
Damage Cost [\$M]	0.554	0.397	0.350	0.351	0.339	0.354	0.336	0.334	
Total LCC [\$M]	1.897	1.754	1.695	1.646	1.614	1.597	1.595	1.593	

Table 7.12 Minimum life cycle cost designs of varied section type numbers with CL-80 set of drift ratio limits and use of sum of initial cost and damage cost as one objective function

# of Section Types	2	3	4	5	6	7	8	
Section Group ID	C1	W14X370	W14X370	W14X370	W14X370	W14X370	W14X257	W14X257
	C2	W14X370	W14X370	W14X370	W14X370	W14X370	W14X370	W14X398
	C3	W14X370	W14X370	W14X370	W14X370	W14X370	W14X370	W14X398
	C4	W14X370	W14X370	W14X370	W14X211	W14X176	W14X193	W14X176
	C5	W14X370	W14X370	W14X370	W14X370	W14X370	W14X370	W14X370
	C6	W14X370	W14X370	W14X370	W14X370	W14X370	W14X370	W14X370
	B1	W36X150	W36X150	W36X150	W36X150	W36X150	W36X150	W36X150
	B2	W36X150	W36X150	W36X150	W36X150	W36X150	W36X150	W36X150
	B3	W36X150	W36X150	W36X150	W36X150	W36X135	W33X130	W36X135
	B4	W36X150	W24X55	W27X84	W27X84	W30X99	W30X99	W30X99
	B5	W36X150	W36X150	W21X62	W21X62	W18X50	W21X44	W21X44
Design Drift Ratio [%]	1.35	1.41	1.30	1.32	1.40	1.39	1.41	
System Yield Coeff.	0.394	0.366	0.367	0.374	0.360	0.348	0.358	
System Overstrength	3.72	3.62	3.60	3.70	3.58	3.56	3.59	
Initial Cost [\$M]	1.415	1.373	1.347	1.295	1.278	1.252	1.259	
Damage Cost [\$M]	0.576	0.464	0.410	0.412	0.396	0.409	0.396	
Total LCC [\$M]	1.991	1.837	1.757	1.707	1.674	1.660	1.655	

Table 7.13 Minimum life cycle cost designs of varied section type numbers with CL-90 set of drift ratio limits and use of sum of initial cost and damage cost as one objective function

# of Section Types	2	3	4	5	6	7	8	9	
Section Group ID	C1	W14X370	W14X370	W14X370	W14X370	W14X370	W14X233	W12X233	W14X233
	C2	W14X370	W14X370	W14X370	W14X370	W14X370	W14X426	W14X426	W14X426
	C3	W14X370	W14X370	W14X370	W14X370	W14X370	W14X426	W14X426	W14X426
	C4	W14X370	W14X370	W14X370	W14X211	W14X176	W14X233	W14X211	W14X193
	C5	W14X370	W14X370	W14X370	W14X370	W14X370	W14X370	W14X370	W14X370
	C6	W14X370	W14X370	W14X370	W14X370	W14X370	W14X370	W14X370	W14X370
	B1	W36X150	W36X150	W36X150	W36X150	W36X150	W36X160	W36X160	W36X150
	B2	W36X150	W36X150	W36X150	W36X150	W36X150	W36X160	W36X160	W36X160
	B3	W36X150	W36X150	W36X150	W36X150	W36X135	W36X135	W36X135	W36X135
	B4	W36X150	W21X68	W27X94	W27X102	W30X99	W30X99	W30X99	W30X99
	B5	W36X150	W36X150	W18X55	W18X50	W18X50	W21X50	W21X50	W21X50
Design Drift Ratio [%]	1.35	1.36	1.37	1.43	1.40	1.33	1.33	1.33	
System Yield Coeff.	0.394	0.369	0.366	0.377	0.360	0.375	0.374	0.369	
System Overstrength	3.72	3.64	3.60	3.72	3.58	3.67	3.67	3.65	
Initial Cost [\$M]	1.415	1.379	1.348	1.297	1.278	1.293	1.285	1.275	
Damage Cost [\$M]	0.727	0.618	0.523	0.525	0.500	0.470	0.473	0.478	
Total LCC [\$M]	2.141	1.963	1.871	1.822	1.778	1.763	1.758	1.754	

Table 7.14 Minimum life cycle cost designs of the same small number of section types and varied sets of drift ratio limits and use of sum of initial cost and damage cost as one objective function

Drift Ratio Limits	CL-40	CL-50	CL-60	CL-70	CL-80	CL-90	
# of Section Types	2	2	2	2	2	2	
Section Group ID	C1	W14X342	W14X342	W14X342	W14X342	W14X370	W14X370
	C2	W14X342	W14X342	W14X342	W14X342	W14X370	W14X370
	C3	W14X342	W14X342	W14X342	W14X342	W14X370	W14X370
	C4	W14X342	W14X342	W14X342	W14X342	W14X370	W14X370
	C5	W14X342	W14X342	W14X342	W14X342	W14X370	W14X370
	C6	W14X342	W14X342	W14X342	W14X342	W14X370	W14X370
	B1	W36X135	W36X135	W36X135	W36X135	W36X150	W36X150
	B2	W36X135	W36X135	W36X135	W36X135	W36X150	W36X150
	B3	W36X135	W36X135	W36X135	W36X135	W36X150	W36X150
	B4	W36X135	W36X135	W36X135	W36X135	W36X150	W36X150
	B5	W36X135	W36X135	W36X135	W36X135	W36X150	W36X150
Design Drift Ratio [%]	1.44	1.44	1.44	1.44	1.35	1.35	
System Yield Coeff.	0.350	0.350	0.350	0.350	0.394	0.394	
System Overstrength	3.51	3.51	3.51	3.51	3.72	3.72	
Initial Cost [\$M]	1.343	1.343	1.343	1.343	1.415	1.415	
Calculated Damage Cost [\$M]	0.377	0.427	0.483	0.554	0.576	0.727	

Table 7.15 Minimum life cycle cost designs of the same medium number of section types and varied sets of drift ratio limits and use of sum of initial cost and damage cost as one objective function

Drift Ratio Limits		CL-40	CL-50	CL-60	CL-70	CL-80	CL-90
# of Section Types		5	5	5	5	5	5
Section Group ID	C1	W14X370	W14X342	W14X370	W14X370	W14X370	W14X370
	C2	W14X370	W14X342	W14X370	W14X370	W14X370	W14X370
	C3	W14X370	W14X342	W14X370	W14X370	W14X370	W14X370
	C4	W14X176	W14X176	W14X176	W14X211	W14X211	W14X211
	C5	W14X370	W14X342	W14X370	W14X370	W14X370	W14X370
	C6	W14X370	W14X342	W14X370	W14X370	W14X370	W14X370
	B1	W36X135	W36X135	W36X135	W36X150	W36X150	W36X150
	B2	W36X135	W36X135	W36X135	W36X150	W36X150	W36X150
	B3	W36X135	W36X135	W36X135	W36X150	W36X150	W36X150
	B4	W27X84	W24X94	W27X84	W24X94	W27X84	W27X102
	B5	W21X50	W21X50	W21X50	W24X55	W21X62	W18X50
Design Drift Ratio [%]		1.43	1.47	1.43	1.35	1.32	1.43
System Yield Coeff.		0.326	0.331	0.326	0.374	0.374	0.377
System Overstrength		3.35	3.49	3.35	3.70	3.70	3.72
Initial Cost [\$M]		1.259	1.232	1.259	1.295	1.295	1.297
Calculated Damage Cost [\$M]		0.253	0.304	0.325	0.351	0.412	0.525

Table 7.16 Globally minimum life cycle cost designs with varied sets of drift ratio limits and use of sum of initial cost and damage cost as one objective function

Drift Ratio Limits	CL-40	CL-50	CL-60	CL-70	CL-80	CL-90	
# of Section Types	8	9	8	9	8	9	
Section Group ID	C1	W14X233	W14X233	W14X257	W14X233	W14X257	W14X233
	C2	W14X370	W14X342	W14X370	W14X426	W14X398	W14X426
	C3	W14X370	W14X370	W14X398	W14X398	W14X398	W14X426
	C4	W14X145	W14X176	W14X176	W14X176	W14X176	W14X193
	C5	W14X342	W14X311	W14X370	W14X370	W14X370	W14X370
	C6	W14X370	W14X311	W14X370	W14X370	W14X370	W14X370
	B1	W36X135	W36X135	W36X150	W36X150	W36X150	W36X150
	B2	W36X135	W36X135	W36X150	W36X150	W36X150	W36X160
	B3	W33X118	W33X130	W33X130	W63X135	W36X135	W36X135
	B4	W27X94	W27X84	W30X99	W30X99	W30X99	W30X99
	B5	W21X44	W21X50	W21X44	W21X44	W21X44	W21X50
Design Drift Ratio [%]	1.48	1.43	1.40	1.42	1.41	1.33	
System Yield Coeff.	0.310	0.319	0.349	0.358	0.358	0.369	
System Overstrength	3.33	3.46	3.56	3.59	3.59	3.65	
Initial Cost [\$M]	1.201	1.188	1.249	1.259	1.259	1.275	
Calculated Damage Cost [\$M]	0.274	0.309	0.301	0.334	0.396	0.478	

Table 7.17 Minimum life cycle cost designs of varied section type number with CL-40 set of drift ratio limits and use of initial cost and damage cost as separate objective functions

# of Section Types	2	3	4	5	6	7	8	9	
Section Group ID	C1	W14X342	W14X342	W14X342	W14X342	W14X283	W12X252	W12X252	W12X279
	C2	W14X342	W14X342	W14X342	W14X342	W14X342	W14X342	W14X342	W14X342
	C3	W14X342	W14X342	W14X342	W14X342	W14X342	W14X342	W14X342	W14X342
	C4	W14X342	W14X342	W14X176	W14X176	W14X176	W14X159	W14X159	W14X159
	C5	W14X342	W14X342	W14X342	W14X342	W14X342	W14X342	W14X311	W14X311
	C6	W14X342	W14X342	W14X342	W14X342	W14X342	W14X342	W14X342	W14X342
	B1	W36X135	W36X135	W36X135	W36X135	W36X135	W36X135	W36X135	W33X130
	B2	W36X135	W36X135	W36X135	W36X135	W36X135	W36X135	W36X135	W36X135
	B3	W36X135	W36X135	W36X135	W36X135	W36X135	W33X118	W33X118	W33X118
	B4	W36X135	W24X68	W24X68	W27X84	W27X84	W27X94	W27X94	W27X84
	B5	W36X135	W24X68	W24X68	W21X50	W18X50	W21X50	W21X50	W21X50
Design Drift Ratio [%]	1.44	1.43	1.52	1.43	1.49	1.39	1.41	1.43	
System Yield Coeff.	0.350	0.328	0.328	0.330	0.326	0.314	0.314	0.304	
System Overstrength	3.51	3.44	3.48	3.46	3.47	3.42	3.42	3.30	
Initial Cost [\$M]	1.343	1.284	1.229	1.228	1.214	1.197	1.187	1.187	
Damage Cost [\$M]	0.377	0.281	0.294	0.272	0.276	0.288	0.288	0.292	
Total LCC [\$M]	1.721	1.565	1.523	1.500	1.490	1.485	1.475	1.479	

Table 7.18 Minimum life cycle cost designs of varied section type number with CL-50 set of drift ratio limits and use of initial cost and damage cost as separate objective functions

# of Section Types	2	3	4	5	6	7	8	9	
Section Group ID	C1	W14X342	W14X342	W14X342	W14X342	W14X283	W14X257	W12X252	W14X283
	C2	W14X342	W14X342	W14X342	W14X342	W14X342	W14X426	W14X370	W14X426
	C3	W14X342	W14X342	W14X342	W14X342	W14X342	W14X342	W14X370	W14X398
	C4	W14X342	W14X342	W14X176	W14X176	W14X176	W14X176	W14X176	W14X176
	C5	W14X342	W14X342	W14X342	W14X342	W14X342	W14X342	W14X342	W14X398
	C6	W14X342	W14X342	W14X342	W14X342	W14X342	W14X342	W14X342	W14X342
	B1	W36X135	W36X135	W36X135	W36X135	W36X135	W36X135	W36X150	W36X150
	B2	W36X135	W36X135	W36X135	W36X135	W36X135	W36X135	W36X135	W36X150
	B3	W36X135	W36X135	W36X135	W36X135	W36X135	W36X135	W36X135	W36X135
	B4	W36X135	W24X68	W24X68	W24X94	W24X94	W24X94	W24X94	W30X99
	B5	W36X135	W24X68	W24X68	W21X50	W18X50	W21X50	W21X50	W18X50
Design Drift Ratio [%]	1.44	1.43	1.52	1.47	1.53	1.48	1.47	1.40	
System Yield Coeff.	0.350	0.328	0.328	0.331	0.327	0.332	0.337	0.360	
System Overstrength	3.51	3.44	3.48	3.49	3.50	3.48	3.56	3.56	
Initial Cost [\$M]	1.343	1.284	1.229	1.232	1.218	1.232	1.226	1.278	
Damage Cost [\$M]	0.427	0.319	0.333	0.304	0.315	0.295	0.294	0.256	
Total LCC [\$M]	1.770	1.603	1.562	1.535	1.533	1.526	1.520	1.534	

Table 7.19 Minimum life cycle cost designs of varied section type number with CL-60 set of drift ratio limits and use of initial cost and damage cost as separate objective functions

# of Section Types	2	3	4	5	6	7	8	9
Section Group ID	C1	W14X342	W14X342	W14X342	W14X342	W14X342	W14X233	W14X233
	C2	W14X342	W14X342	W14X342	W14X342	W14X342	W14X426	W14X426
	C3	W14X342	W14X342	W14X342	W14X342	W14X342	W14X426	W14X426
	C4	W14X342	W14X342	W14X176	W14X176	W14X233	W14X233	W14X193
	C5	W14X342	W14X342	W14X342	W14X342	W14X342	W14X370	W14X370
	C6	W14X342	W14X342	W14X342	W14X342	W14X342	W14X342	W14X342
	B1	W36X135	W36X135	W36X135	W36X135	W36X135	W36X160	W36X160
	B2	W36X135	W36X135	W36X135	W36X135	W36X135	W36X160	W36X135
	B3	W36X135	W36X135	W36X135	W36X135	W33X118	W36X135	W36X135
	B4	W36X135	W24X68	W24X68	W21X111	W21X111	W30X99	W30X99
	B5	W36X135	W24X68	W24X68	W18X55	W21X50	W21X50	W21X50
Design Drift Ratio [%]	1.44	1.43	1.52	1.50	1.48	1.34	1.33	1.33
System Yield Coeff.	0.350	0.328	0.328	0.335	0.312	0.373	0.374	0.355
System Overstrength	3.51	3.44	3.48	3.54	3.32	3.68	3.67	3.55
Initial Cost [\$M]	1.343	1.284	1.229	1.241	1.251	1.279	1.288	1.264
Damage Cost [\$M]	0.483	0.362	0.378	0.356	0.350	0.285	0.277	0.320
Total LCC [\$M]	1.827	1.646	1.607	1.597	1.601	1.563	1.565	1.584

Table 7.20 Minimum life cycle cost designs of varied section type number with CL-70 set of drift ratio limits and use of initial cost and damage cost as separate objective functions

# of Section Types	2	3	4	5	6	7	8	9	
Section Group ID	C1	W14X342	W14X342	W14X342	W14X342	W12X279	W12X252	W12X252	W12X252
	C2	W14X342	W14X342	W14X342	W14X342	W14X342	W14X398	W14X342	W14X398
	C3	W14X342	W14X342	W14X342	W14X342	W14X342	W14X398	W14X342	W14X426
	C4	W14X342	W14X342	W14X176	W14X176	W14X176	W14X211	W14X145	W14X176
	C5	W14X342	W14X342	W14X342	W14X342	W14X342	W14X398	W14X342	W14X398
	C6	W14X342	W14X342	W14X342	W14X342	W14X342	W14X398	W14X311	W14X398
	B1	W36X135	W36X135	W36X135	W36X135	W36X135	W36X160	W36X135	W36X160
	B2	W36X135	W36X135	W36X135	W36X135	W36X135	W36X160	W36X135	W36X150
	B3	W36X135	W36X135	W36X135	W36X135	W36X135	W36X135	W33X118	W33X130
	B4	W36X135	W24X68	W24X68	W24X76	W24X76	W27X94	W24X94	W27X94
	B5	W36X135	W24X68	W24X68	W24X62	W24X55	W24X55	W24X55	W21X62
Design Drift Ratio [%]	1.44	1.43	1.52	1.47	1.45	1.27	1.43	1.33	
System Yield Coeff.	0.350	0.328	0.328	0.329	0.322	0.369	0.313	0.349	
System Overstrength	3.51	3.44	3.48	3.47	3.48	3.68	3.41	3.58	
Initial Cost [\$M]	1.343	1.284	1.229	1.230	1.211	1.293	1.190	1.281	
Damage Cost [\$M]	0.554	0.415	0.434	0.414	0.414	0.333	0.428	0.349	
Total LCC [\$M]	1.897	1.699	1.663	1.643	1.625	1.626	1.617	1.631	

Table 7.21 Minimum life cycle cost designs of varied section type number with CL-80 set of drift ratio limits and use of initial cost and damage cost as separate objective functions

# of Section Types	2	3	4	5	6	7	8	9	
Section Group ID	C1	W14X370	W14X342	W14X342	W14X342	W14X370	W14X370	W14X311	W12X252
	C2	W14X370	W14X342	W14X342	W14X342	W14X370	W14X370	W14X426	W14X426
	C3	W14X370	W14X342	W14X342	W14X342	W14X370	W14X370	W14X426	W14X426
	C4	W14X370	W14X342	W14X176	W14X176	W14X176	W14X193	W14X233	W14X211
	C5	W14X370	W14X342	W14X342	W14X342	W14X370	W14X342	W14X370	W14X370
	C6	W14X370	W14X342	W14X342	W14X342	W14X370	W14X342	W14X370	W14X370
	B1	W36X150	W36X135	W36X135	W36X135	W36X150	W36X150	W36X150	W36X170
	B2	W36X150	W36X135	W36X135	W36X135	W36X150	W36X135	W36X150	W36X160
	B3	W36X150	W36X135	W36X135	W36X135	W36X135	W36X135	W36X135	W36X150
	B4	W36X150	W24X68	W24X68	W24X76	W27X94	W30X99	W27X94	W27X94
	B5	W36X150	W24X68	W24X68	W24X62	W24X62	W16X50	W24X62	W24X55
Design Drift Ratio [%]	1.35	1.43	1.52	1.47	1.31	1.46	1.30	1.28	
System Yield Coeff.	0.394	0.328	0.328	0.329	0.364	0.345	0.366	0.393	
System Overstrength	3.72	3.44	3.48	3.47	3.61	3.48	3.57	3.83	
Initial Cost [\$M]	1.415	1.284	1.229	1.230	1.281	1.263	1.306	1.300	
Damage Cost [\$M]	0.576	0.489	0.511	0.487	0.410	0.435	0.397	0.379	
Total LCC [\$M]	1.991	1.773	1.740	1.717	1.691	1.698	1.703	1.679	

Table 7.22 Minimum life cycle cost designs of varied section type number with CL-90 set of drift ratio limits and use of initial cost and damage cost as separate objective functions

# of Section Types	2	3	4	5	6	7	8	9	
Section Group ID	C1	W14X370	W14X342	W14X426	W14X398	W14X398	W14X257	W12X252	W14X257
	C2	W14X370	W14X342	W14X426	W14X398	W14X426	W14X398	W14X398	W14X426
	C3	W14X370	W14X342	W14X426	W14X398	W14X426	W14X398	W14X398	W14X398
	C4	W14X370	W14X342	W14X233	W14X211	W14X211	W14X176	W14X176	W14X211
	C5	W14X370	W14X342	W14X426	W14X398	W14X398	W14X398	W14X342	W14X342
	C6	W14X370	W14X342	W14X426	W14X398	W14X398	W14X398	W14X342	W14X398
	B1	W36X150	W36X135	W36X170	W36X150	W36X160	W36X150	W36X150	W36X150
	B2	W36X150	W36X135	W36X170	W36X150	W36X160	W36X150	W36X150	W36X150
	B3	W36X150	W36X135	W36X170	W36X150	W36X160	W36X135	W36X135	W36X135
	B4	W36X150	W24X68	W27X84	W27X94	W27X94	W27X94	W27X94	W27X94
	B5	W36X150	W24X68	W27X84	W24X55	W24X55	W18X55	W21X50	W24X55
Design Drift Ratio [%]	1.35	1.43	1.26	1.27	1.30	1.40	1.40	1.31	
System Yield Coeff.	0.394	0.328	0.438	0.377	0.397	0.353	0.356	0.360	
System Overstrength	3.72	3.44	3.98	3.63	3.72	3.55	3.65	3.58	
Initial Cost [\$M]	1.415	1.284	1.398	1.326	1.349	1.275	1.243	1.275	
Damage Cost [\$M]	0.727	0.618	0.469	0.487	0.454	0.506	0.529	0.499	
Total LCC [\$M]	2.141	1.902	1.867	1.814	1.803	1.780	1.772	1.774	

Table 7.23 Designs of five section types with similar calculated damage cost using varied sets of drift ratio limits

Drift Ratio Limits	CL-40	CL-50	CL-60	CL-70	CL-80	CL-90	
# of Section Types	5	5	5	5	5	5	
Section Group ID	C1	W14X257	W14X342	W14X370	W14X455	W14X500	W14X605
	C2	W14X342	W14X342	W14X370	W14X455	W14X500	W14X605
	C3	W14X342	W14X342	W14X426	W14X398	W14X500	W14X605
	C4	W14X176	W14X176	W14X370	W14X398	W14X342	W14X500
	C5	W14X342	W14X342	W14X370	W14X398	W14X500	W14X605
	C6	W14X342	W14X342	W14X370	W14X398	W14X500	W14X605
	B1	W36X135	W36X135	W36X150	W36X160	W36X210	W36X245
	B2	W36X135	W36X135	W36X150	W36X160	W36X210	W36X245
	B3	W36X135	W36X135	W36X150	W36X160	W36X150	W36X150
	B4	W24X68	W24X94	W30X99	W27X102	W36X150	W36X150
	B5	W24X68	W21X50	W16X57	W24X55	W21X44	W24X55
Design Drift Ratio [%]	1.50	1.47	1.34	1.25	1.19	1.04	
System Yield Coeff.	0.325	0.331	0.373	0.405	0.508	0.556	
System Overstrength	3.51	3.49	3.62	3.70	4.15	4.13	
Initial Cost [\$M]	1.209	1.232	1.358	1.432	1.552	1.754	
Calculated Damage Cost [\$M]	0.295	0.304	0.301	0.301	0.293	0.295	

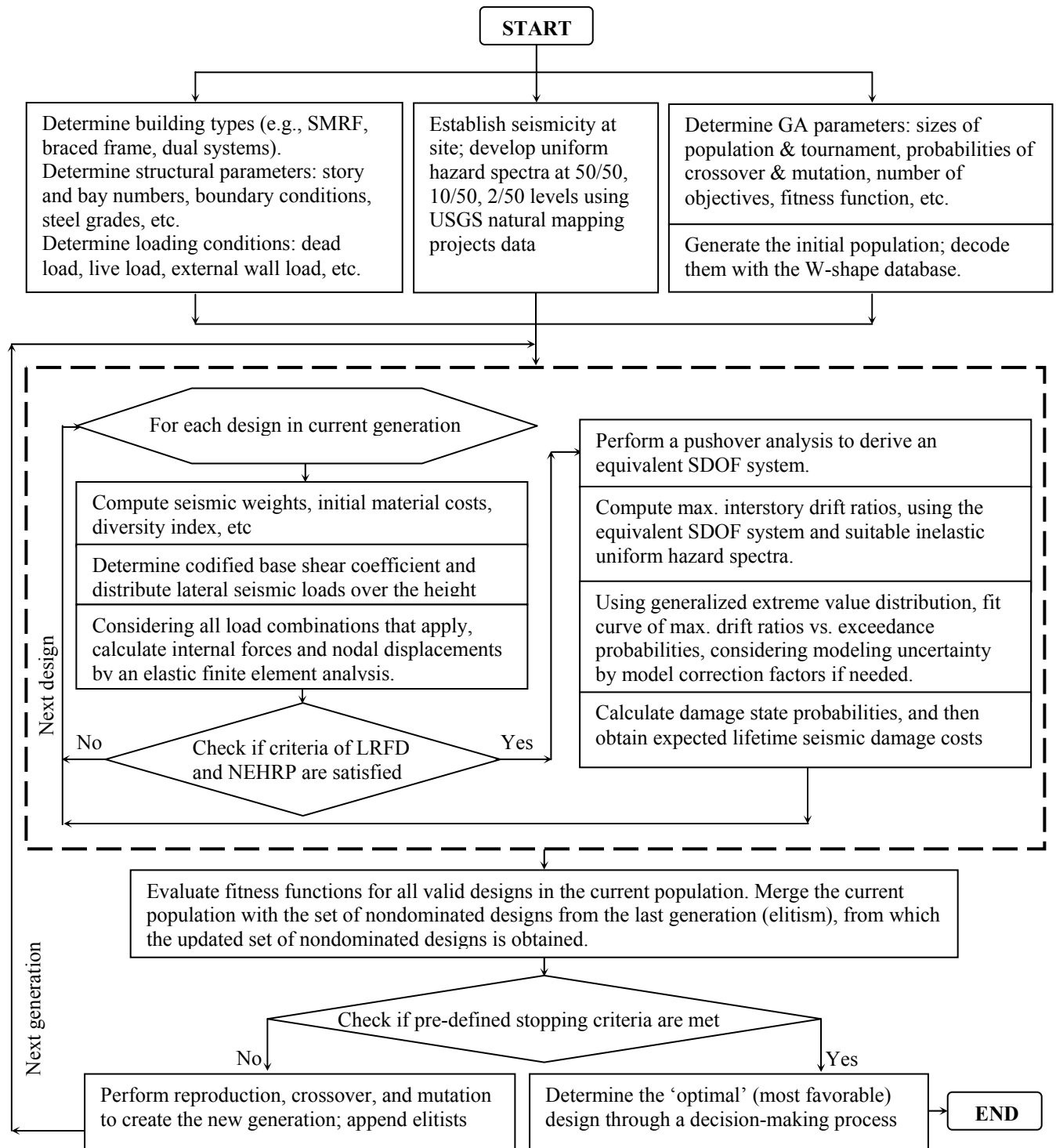


Figure 7.1 Flowchart of the proposed GA-based multiobjective optimization procedure for designing steel SMRF structures considering life cycle costs

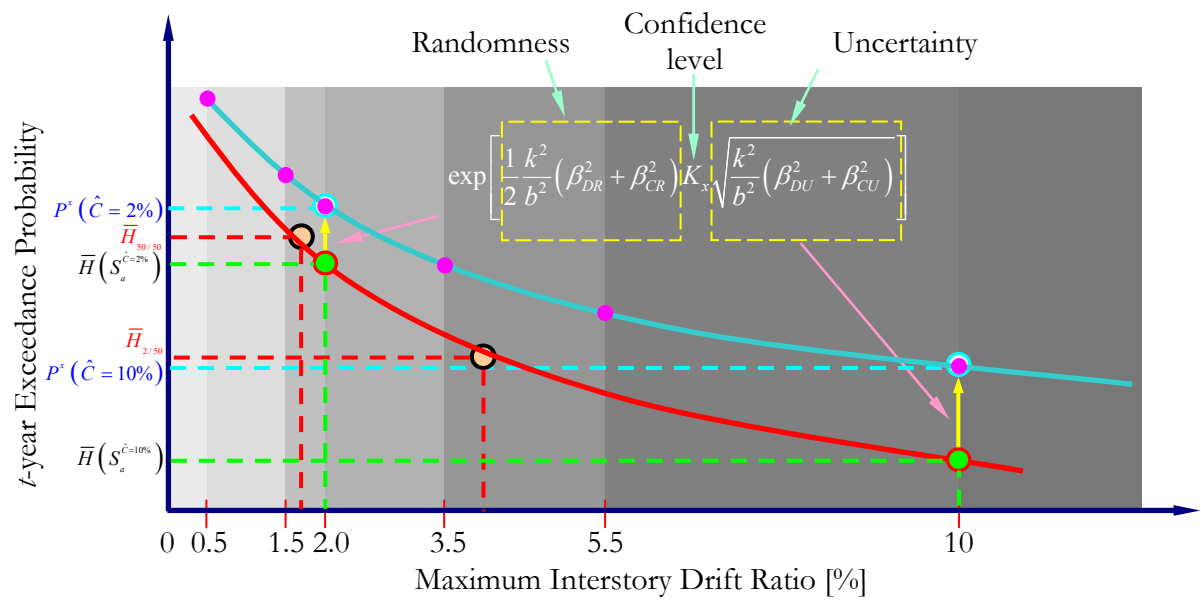


Figure 7.2 Incorporation of randomness/uncertainty by increasing exceedance probability

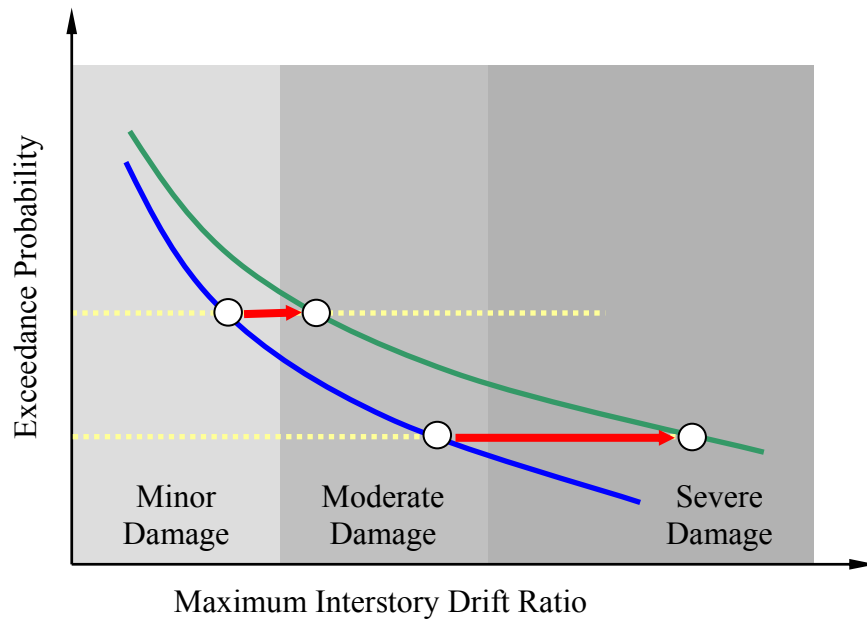


Figure 7.3 Incorporation of randomness/uncertainty by increasing drift ratio demands

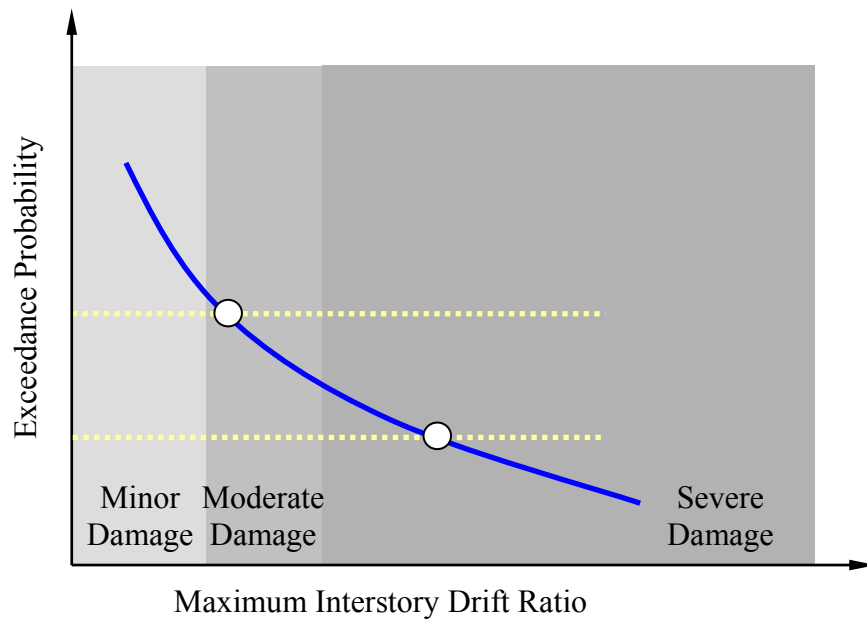


Figure 7.4 Incorporation of randomness/uncertainty by decreasing drift ratio limits that define damage states

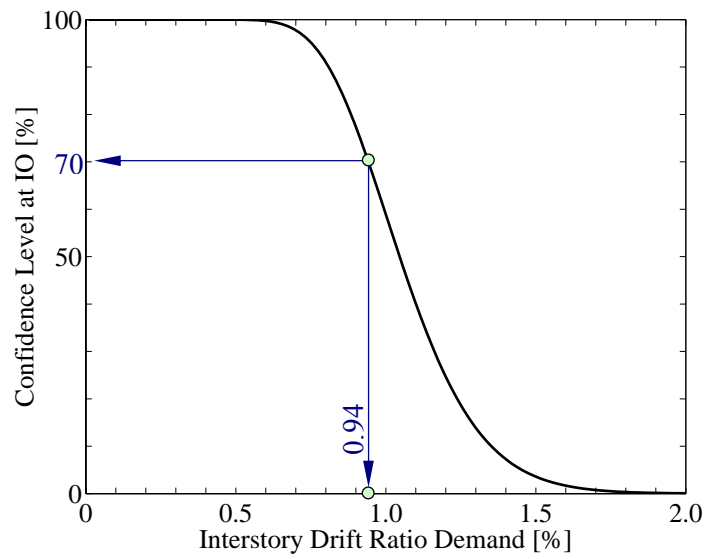


Figure 7.5 Confidence level curve for Immediate Occupancy drift ratio limit

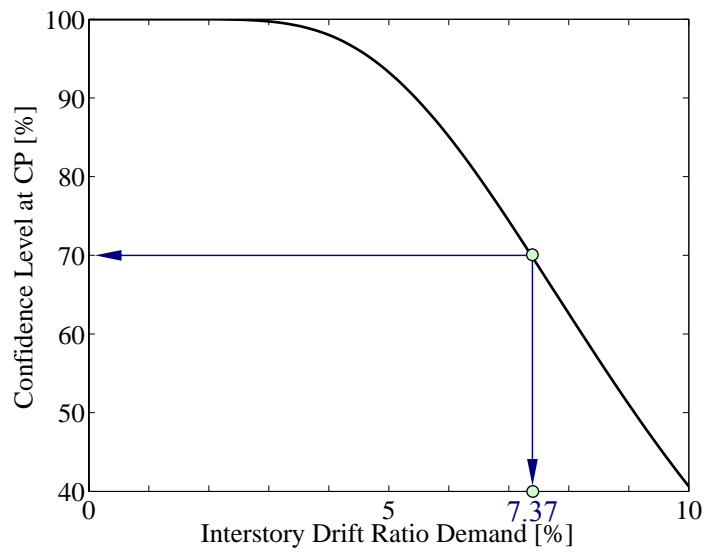


Figure 7.6 Confidence level curve for Collapse Prevention drift ratio limit

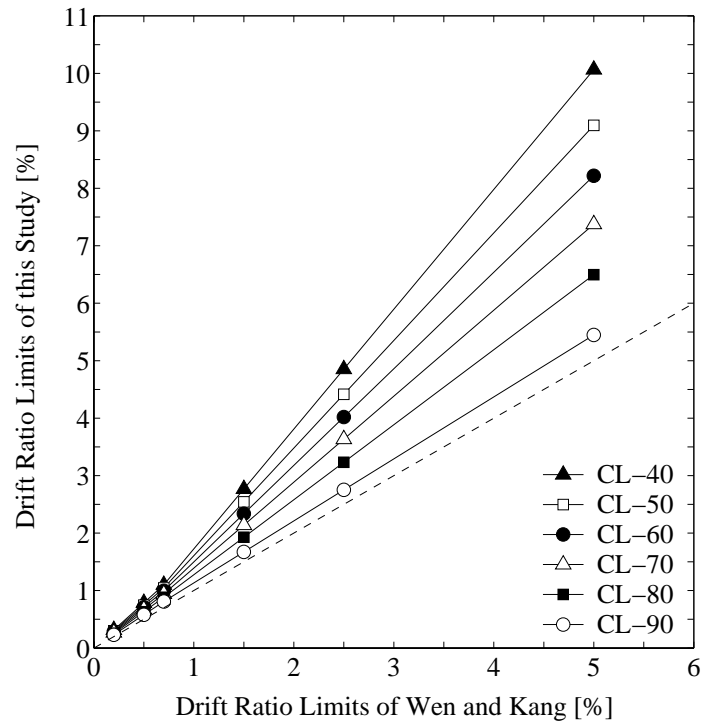


Figure 7.7 Comparison of varied confidence level dependent sets of drift ratio limits

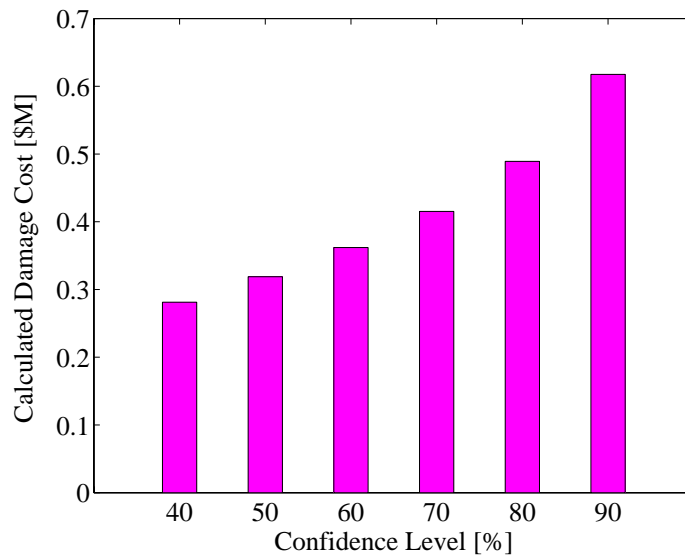


Figure 7.8 Varied calculated damage costs for the same SMRF design using varied confidence level dependent sets of drift ratio limits

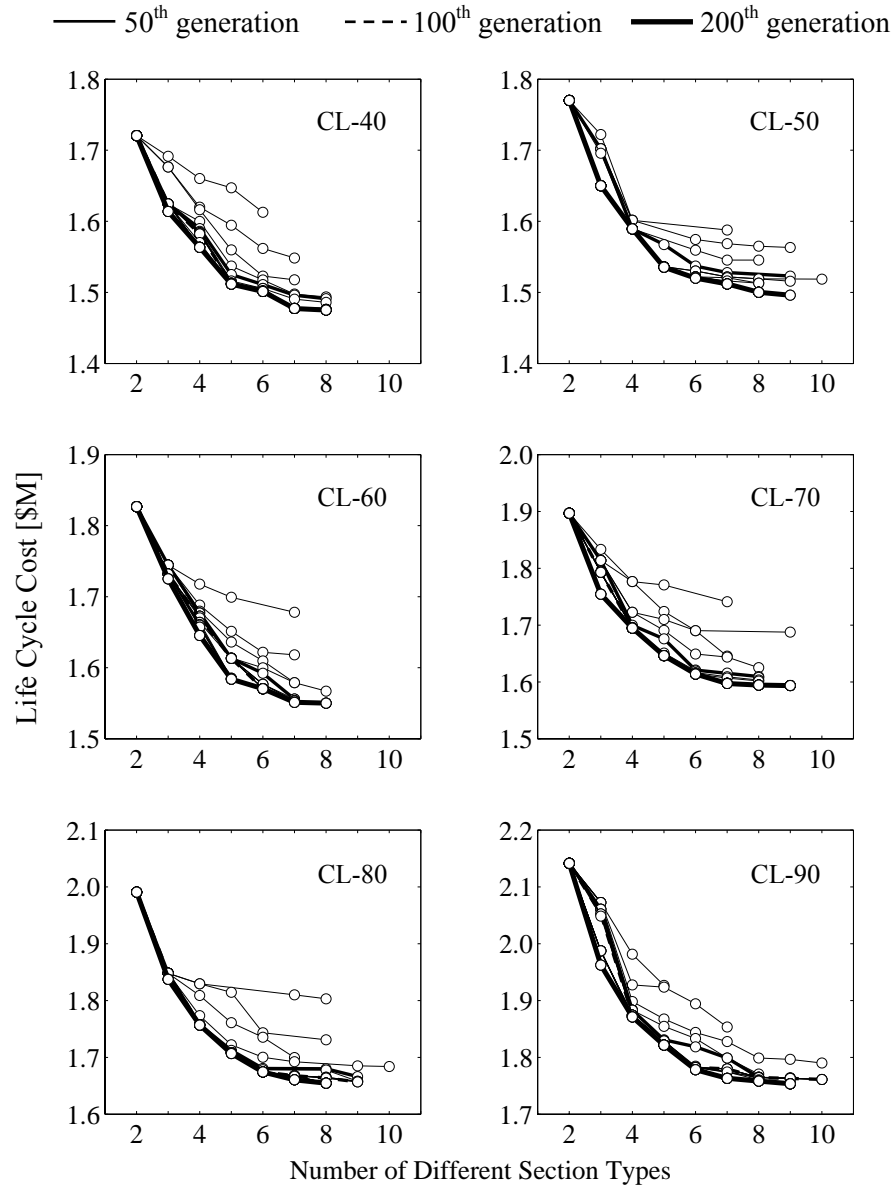


Figure 7.9 Generational evolution of optimized designs using varied confidence level dependent sets of drift ratio limits

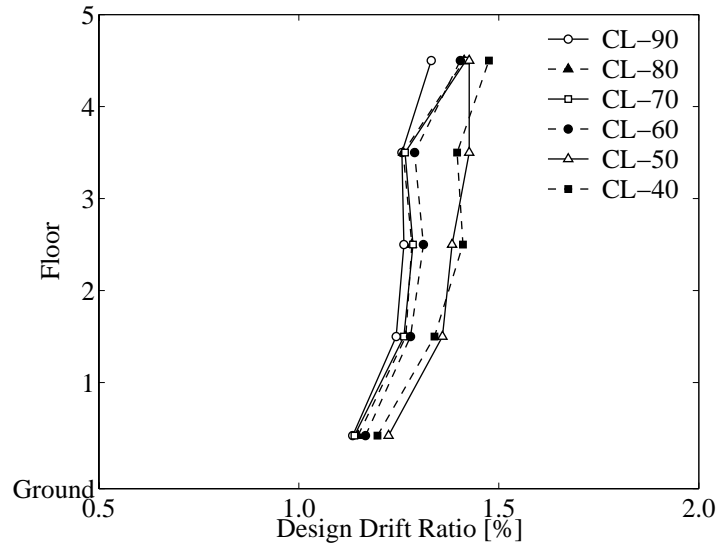


Figure 7.10 Nominal design drift ratio profiles for globally minimum life cycle cost designs obtained using varied confidence level dependent sets of drift ratio limits

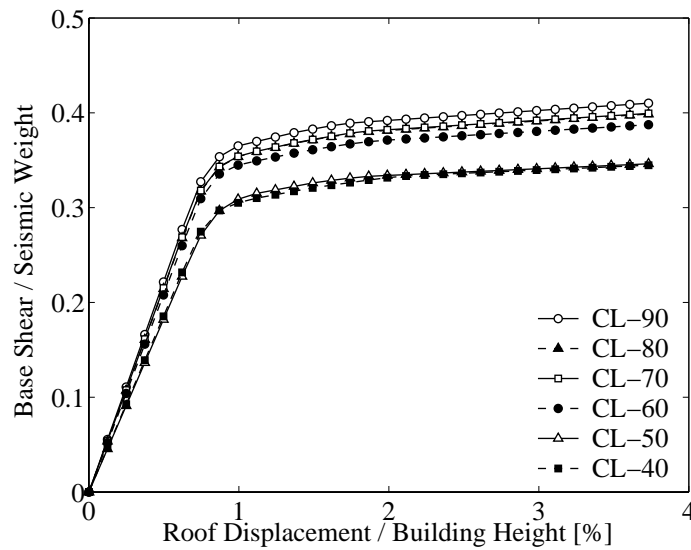


Figure 7.11 Normalized static pushover curves for globally minimum life cycle cost designs obtained using varied confidence level dependent sets of drift ratio limits

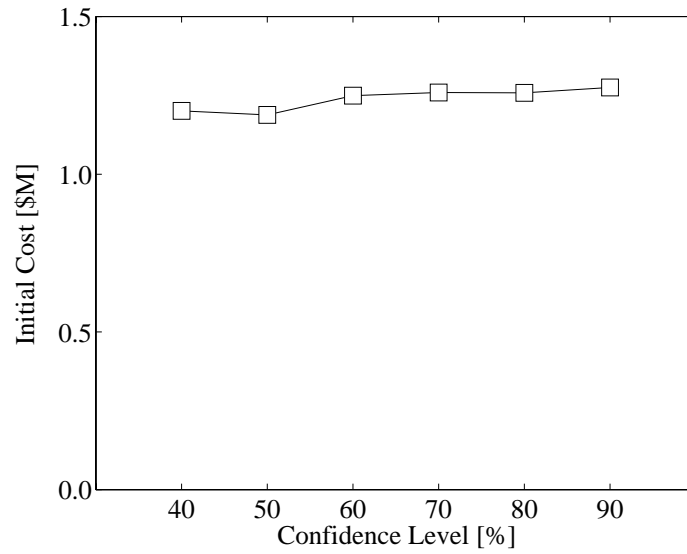


Figure 7.12 Initial costs for globally minimum life cycle cost designs obtained using varied confidence level dependent sets of drift ratio limits

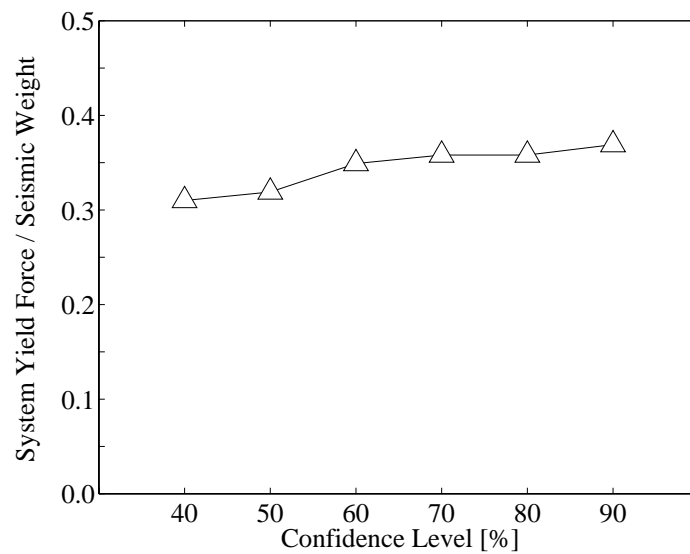


Figure 7.13 Actual system yield levels for globally minimum life cycle cost designs obtained using varied confidence level dependent sets of drift ratio limits

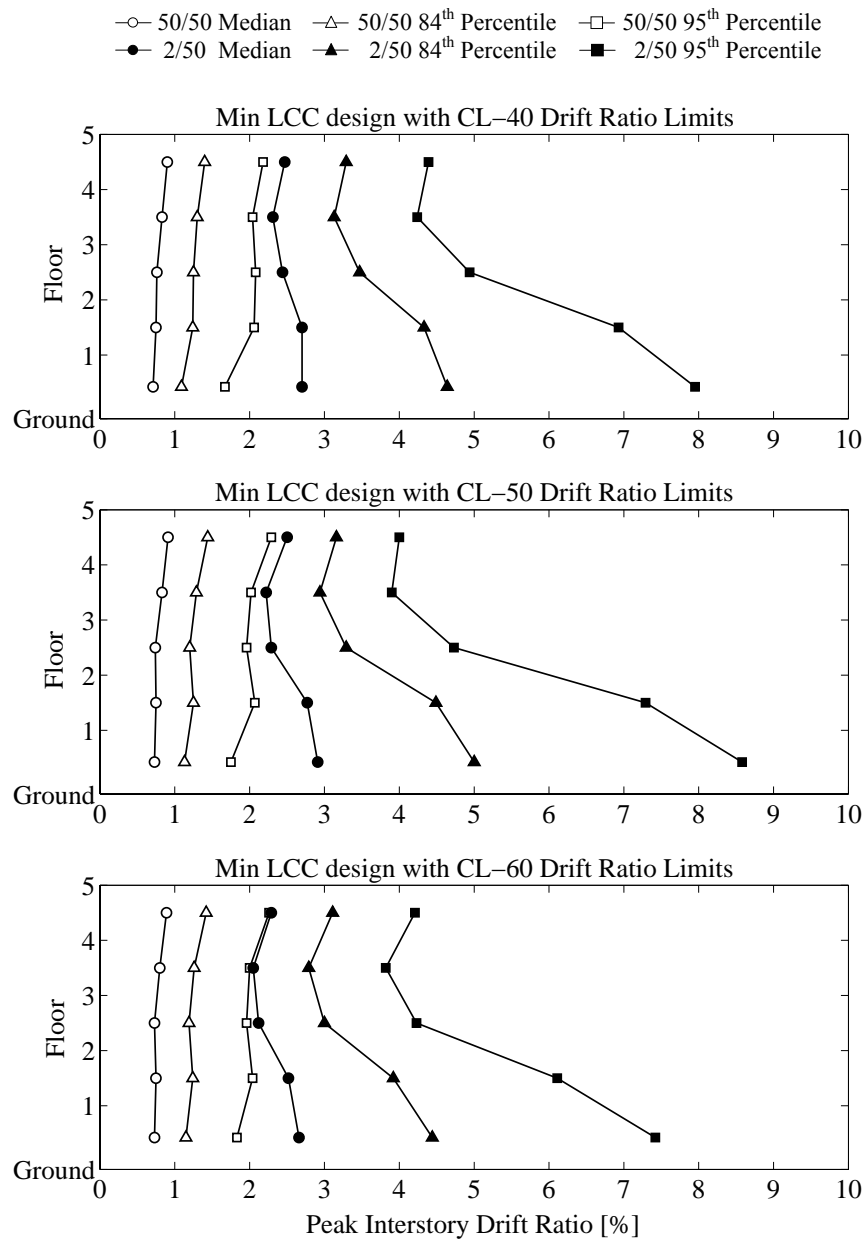


Figure 7.14 Peak interstory drift demand profiles at different hazard levels by time history analysis for globally minimum life cycle cost designs obtained using varied confidence level dependent sets of drift ratio limits

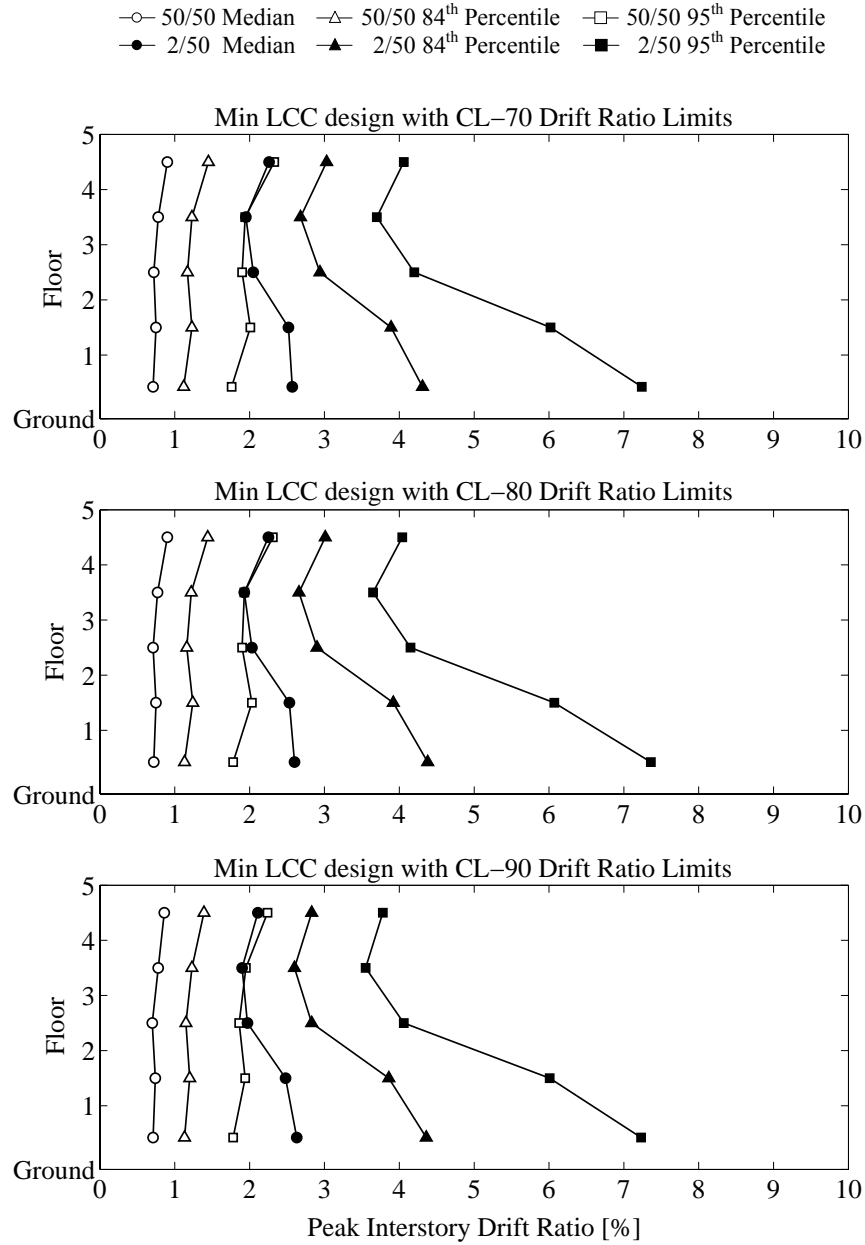


Figure 7.14 (cont'd) Peak interstory drift demand profiles at different hazard levels by time history analysis for globally minimum life cycle cost designs obtained using varied confidence level dependent sets of drift ratio limits

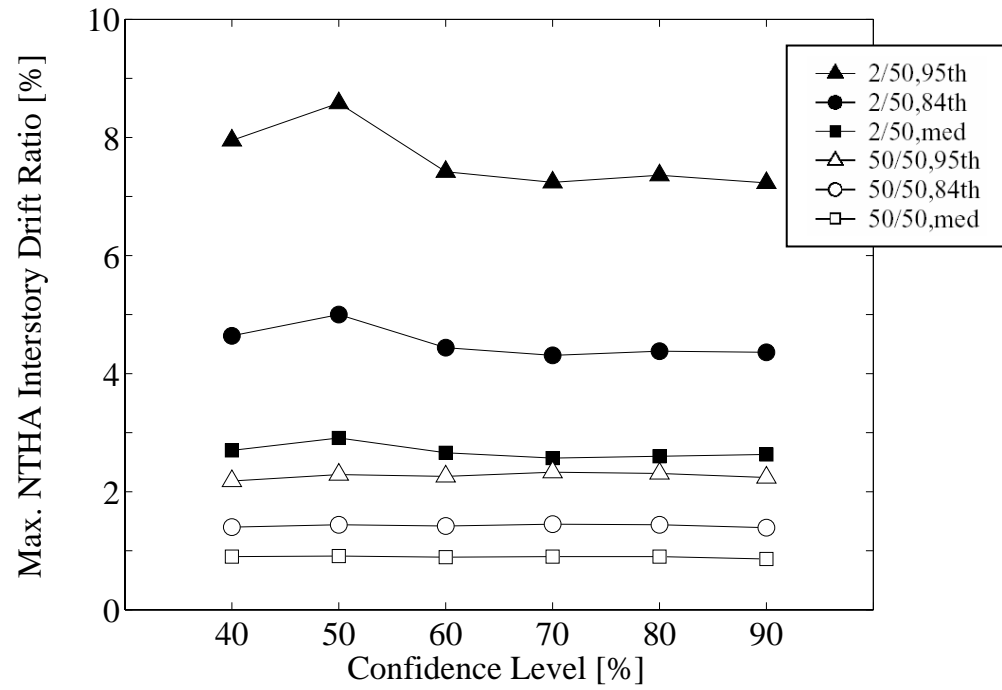


Figure 7.15 Maximum peak interstory drift demands at different hazard levels by time history analysis for globally minimum life cycle cost designs obtained using varied confidence level dependent sets of drift ratio limits

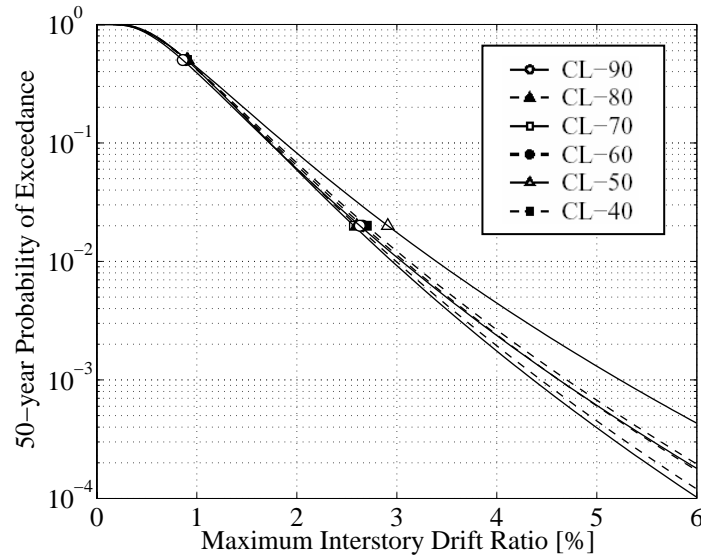


Figure 7.16 Median 50-year probabilistic performance curves by time history analysis for globally minimum life cycle cost designs obtained using varied sets of drift ratio limits

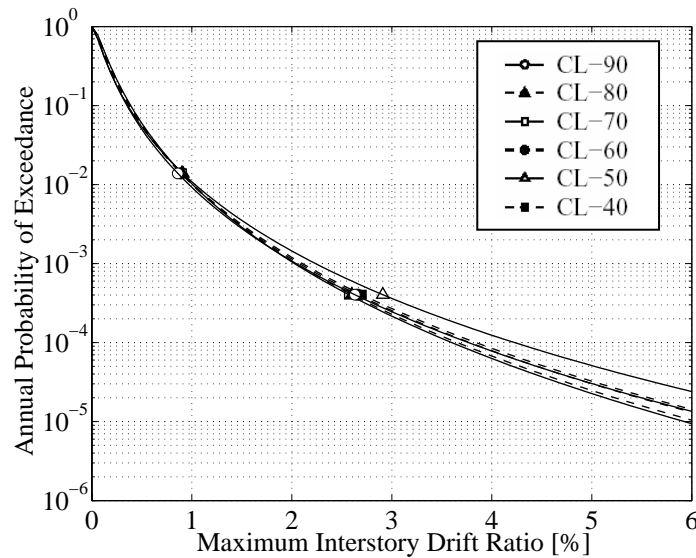


Figure 7.17 Median annual probabilistic performance curves by time history analysis for globally minimum life cycle cost designs obtained using varied sets of drift ratio limits

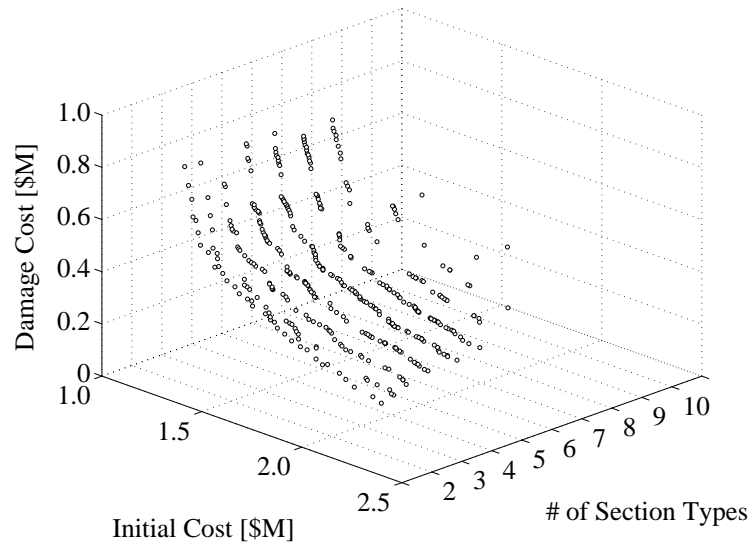


Figure 7.18 3D tradeoff among objective functions for all 398 optimized designs at the 200th generation with CL-70 set of drift ratio limits

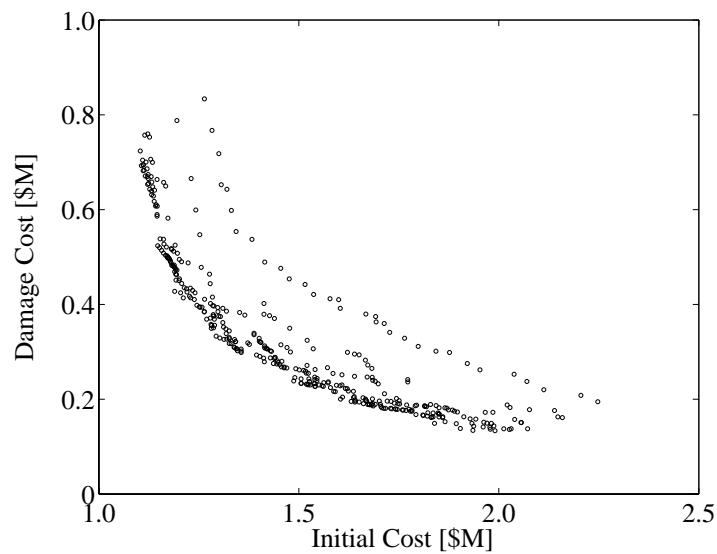


Figure 7.19 2D projection of tradeoff among objective functions for all 398 optimized designs at the 200th generation with CL-70 set of drift ratio limits

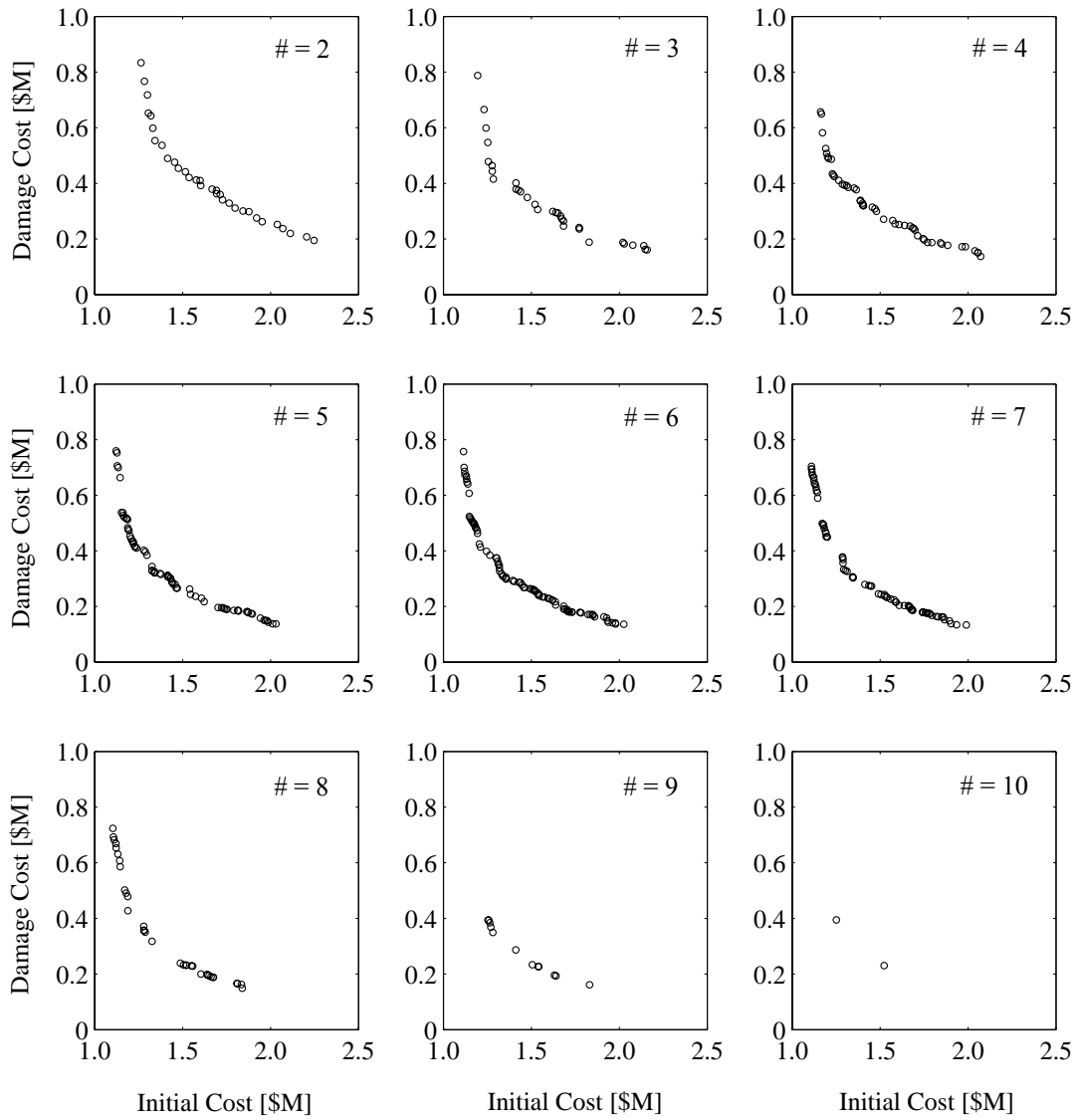


Figure 7.20 Tradeoff among initial cost and damage cost for each section type number using all 398 optimized designs at the 200th generation with CL-70 set of drift ratio limits

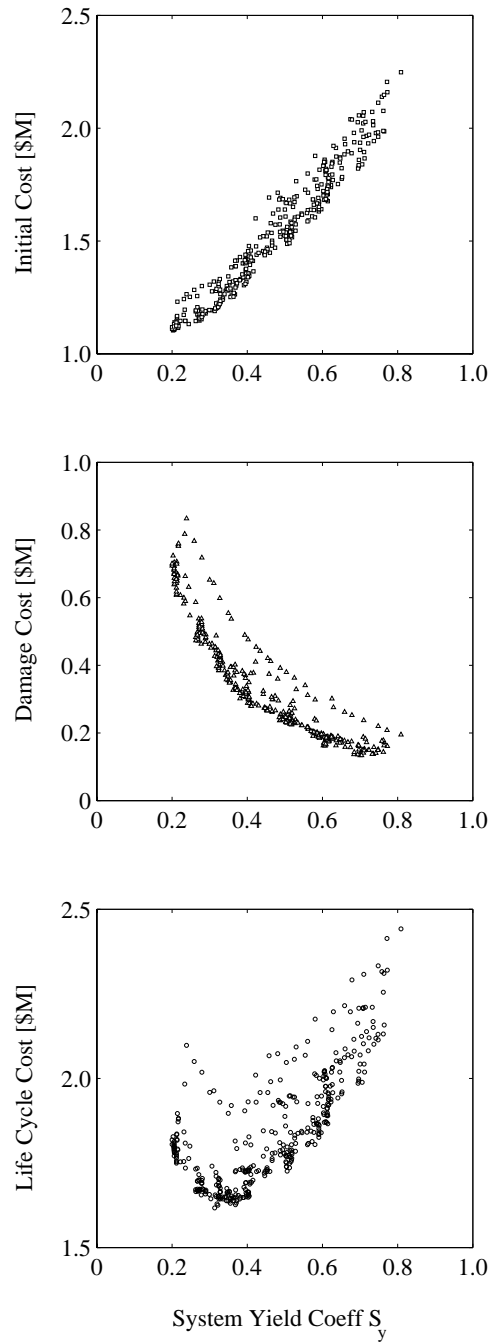


Figure 7.21 Monetary costs as a function of system yield coefficient for all 398 optimized designs at the 200th generation with CL-70 set of drift ratio limits

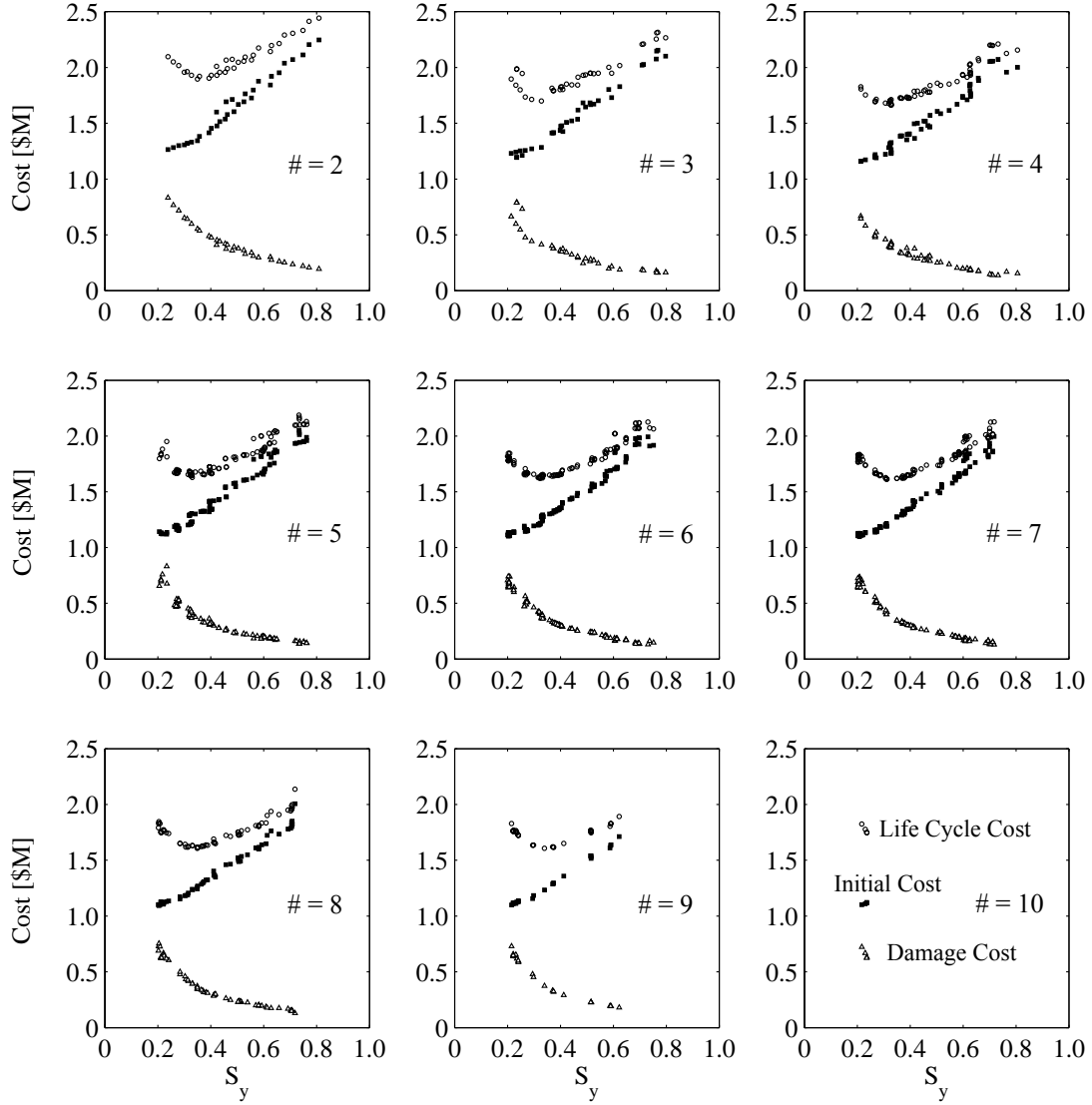


Figure 7.22 Monetary costs as a function of system yield coefficient for each section type number using all 398 optimized designs at the 200th generation with CL-70 set of drift ratio limits

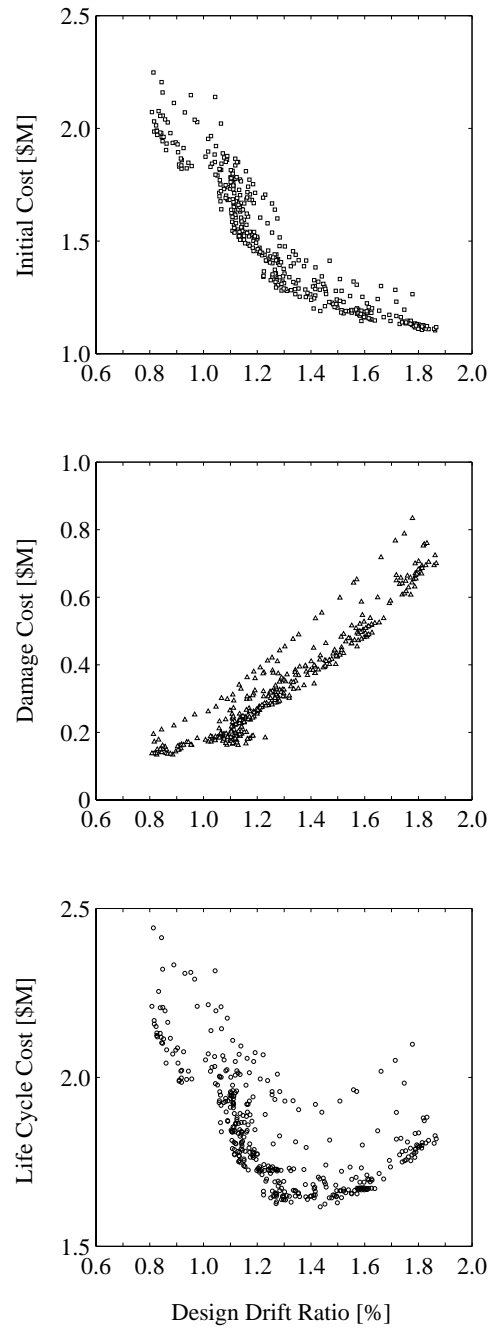


Figure 7.23 Monetary costs as a function of design drift ratio for all 398 optimized designs at the 200th generation with CL-70 set of drift ratio limits

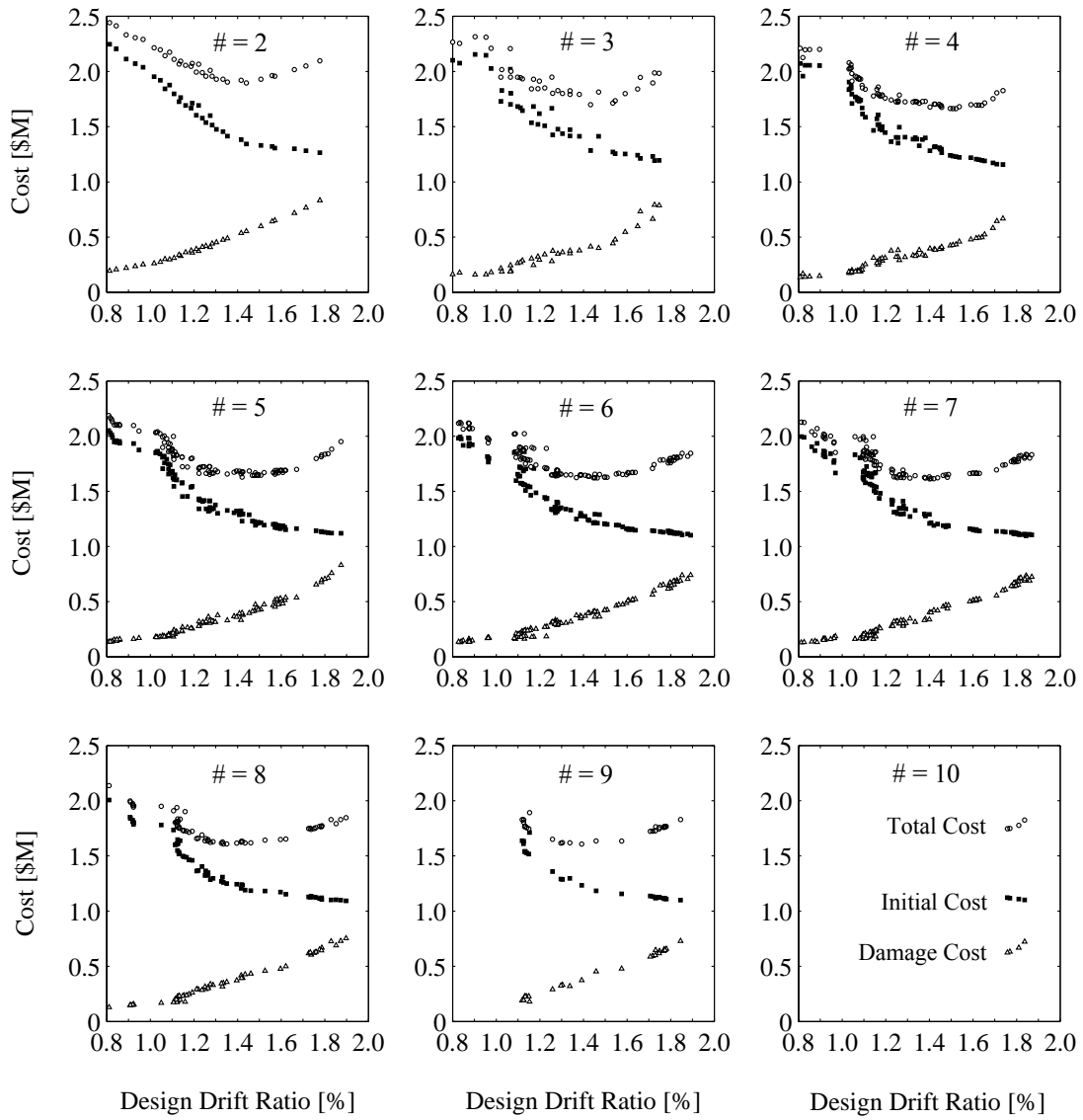


Figure 7.24 Costs as a function of design drift ratio for each section type number using all 398 optimized designs at the 200th generation with CL-70 set of drift ratio limits

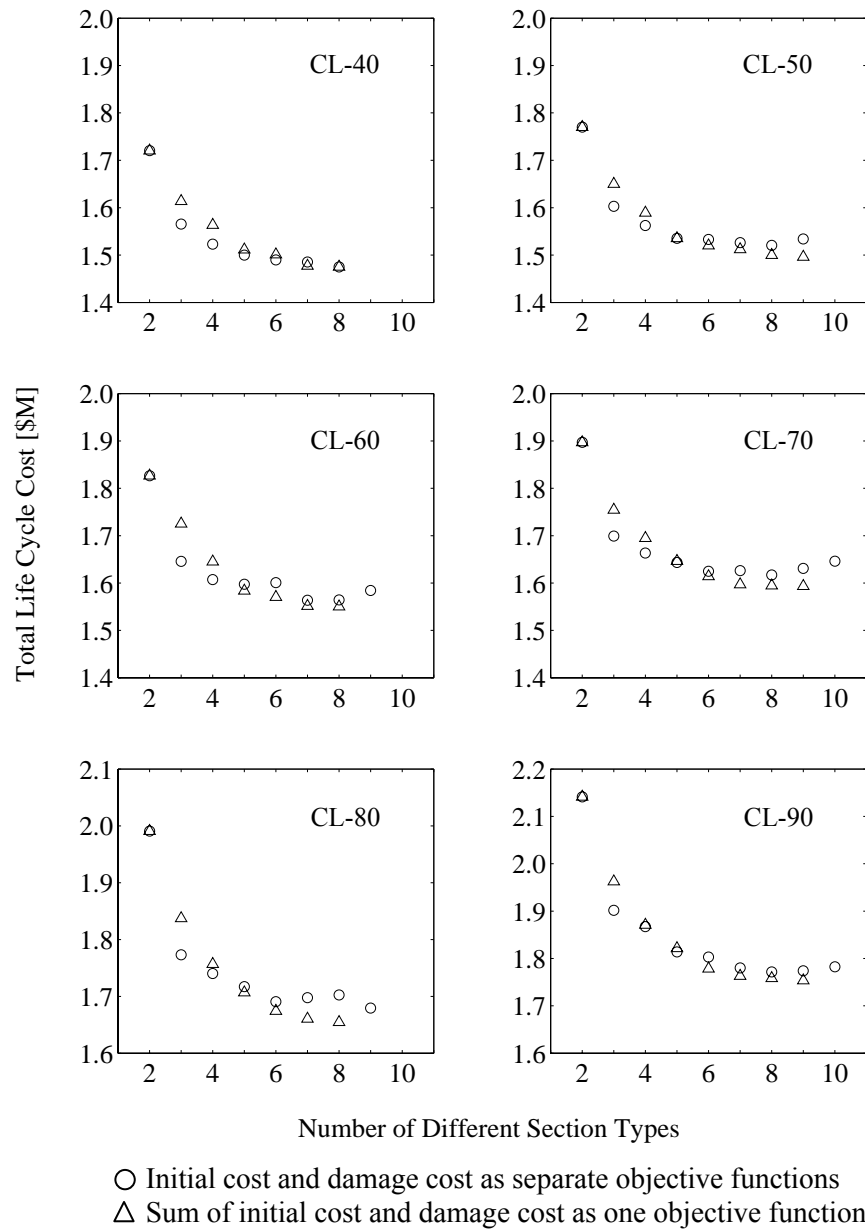


Figure 7.25 Comparison of minimum life cycle cost designs at the 200th generation

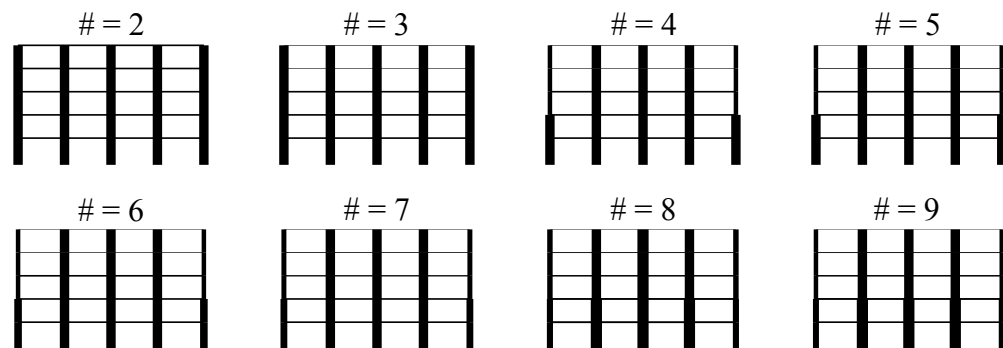


Figure 7.26 Sketches of minimum life cycle cost designs of varied section type numbers at the 200th generation with CL-70 set of drift ratio limits

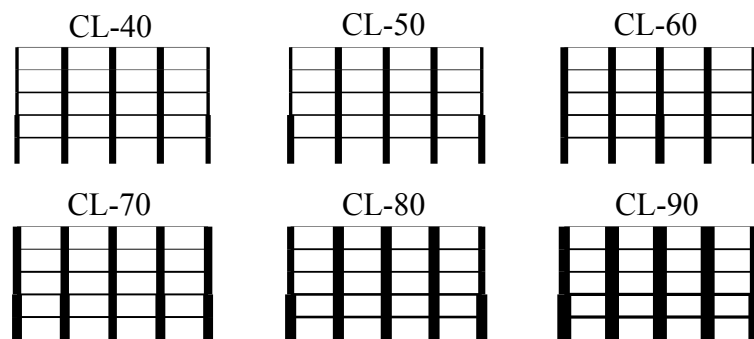


Figure 7.27 Sketches for design solutions of five section types with similar calculated damage cost obtained using varied confidence level dependent sets of drift ratio limits

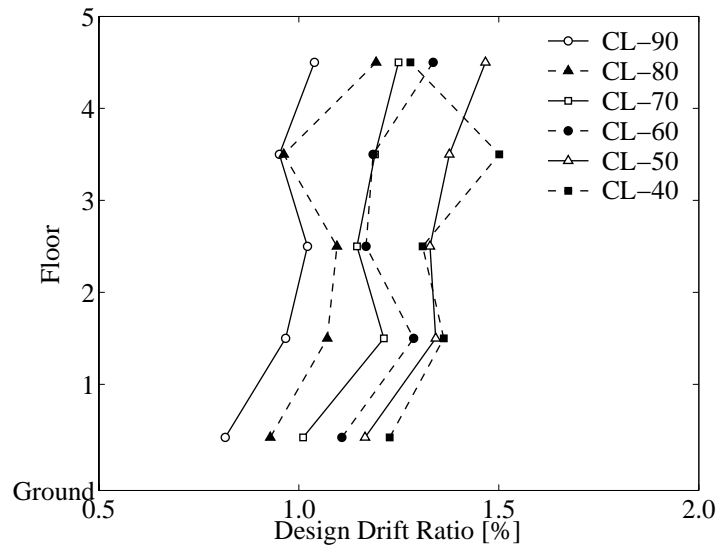


Figure 7.28 Nominal design drift ratio profiles for design solutions of five section types with similar calculated damage cost obtained using varied confidence level dependent sets of drift ratio limits

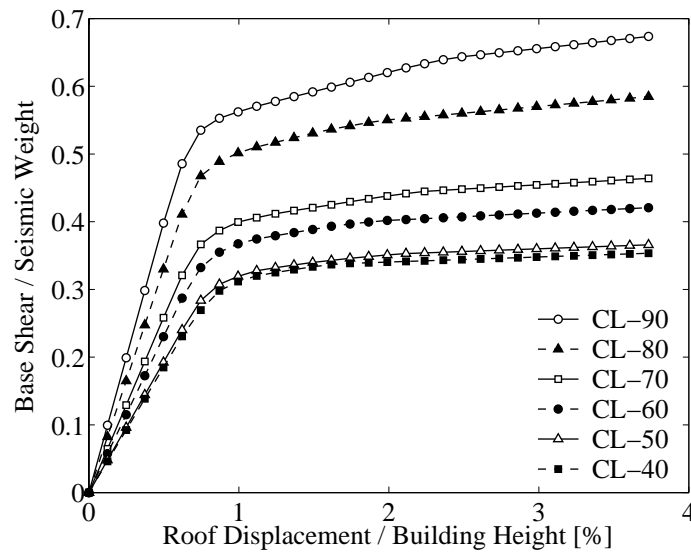


Figure 7.29 Normalized static pushover curves for design solutions of five section types with similar calculated damage cost obtained using varied confidence level dependent sets of drift ratio limits

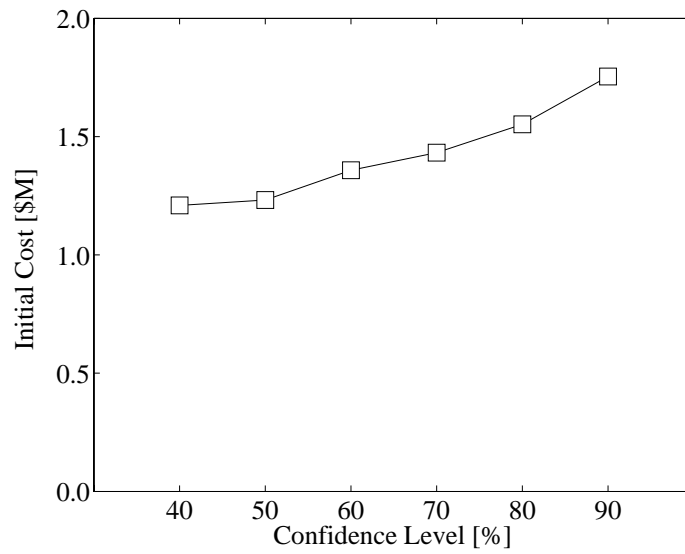


Figure 7.30 Initial costs for design solutions of five section types with similar calculated damage cost obtained using varied confidence level dependent sets of drift ratio limits

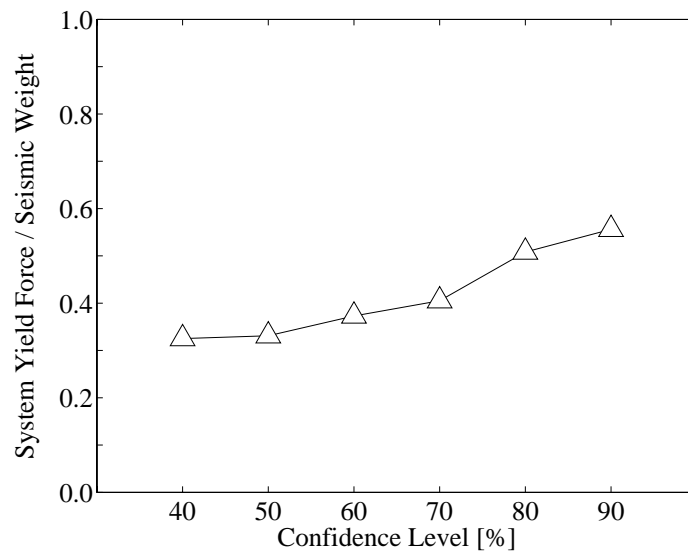


Figure 7.31 Actual system yield levels for design solutions of five section types with similar calculated damage cost obtained using varied confidence level dependent sets of drift ratio limits

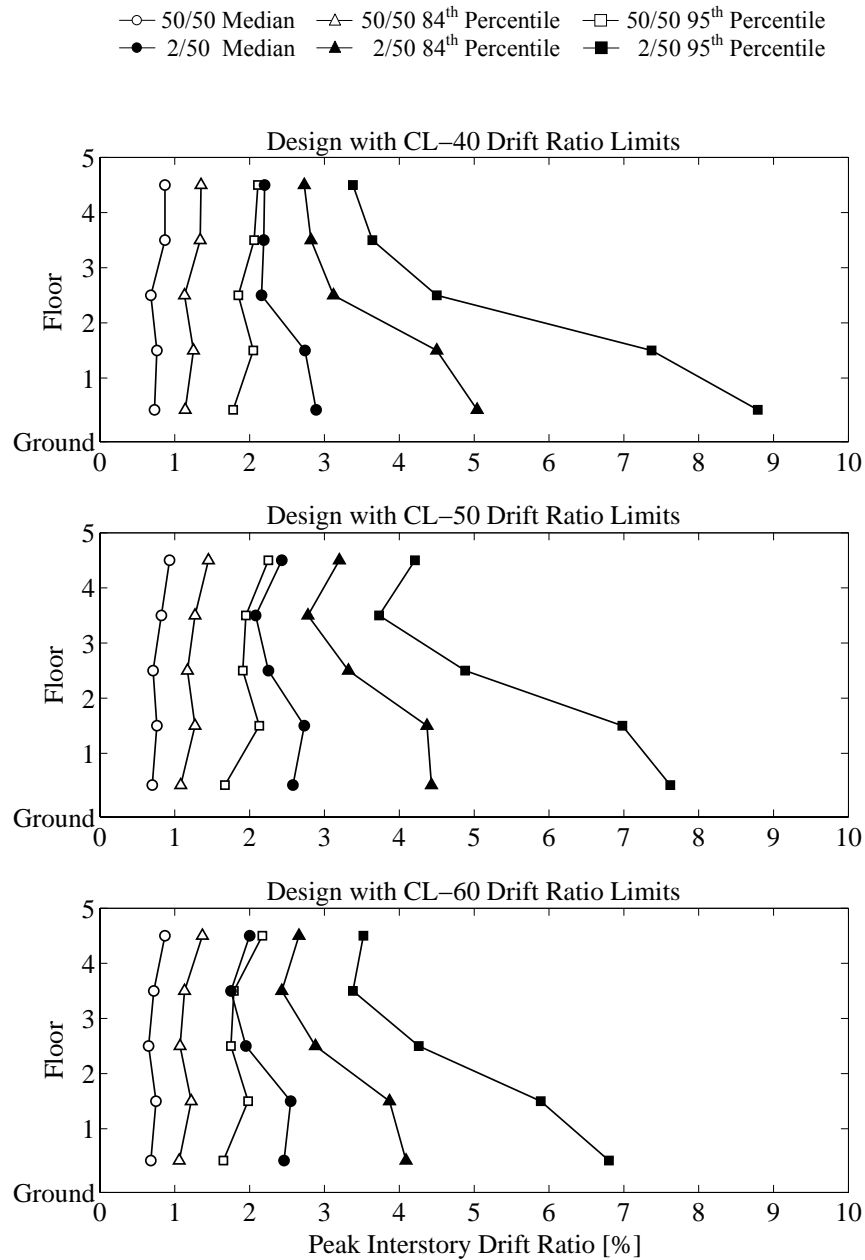


Figure 7.32 Peak interstory drift demand profiles at different hazard levels by time history analysis for design solutions of five section types with similar calculated damage cost obtained using varied confidence level dependent sets of drift ratio limits

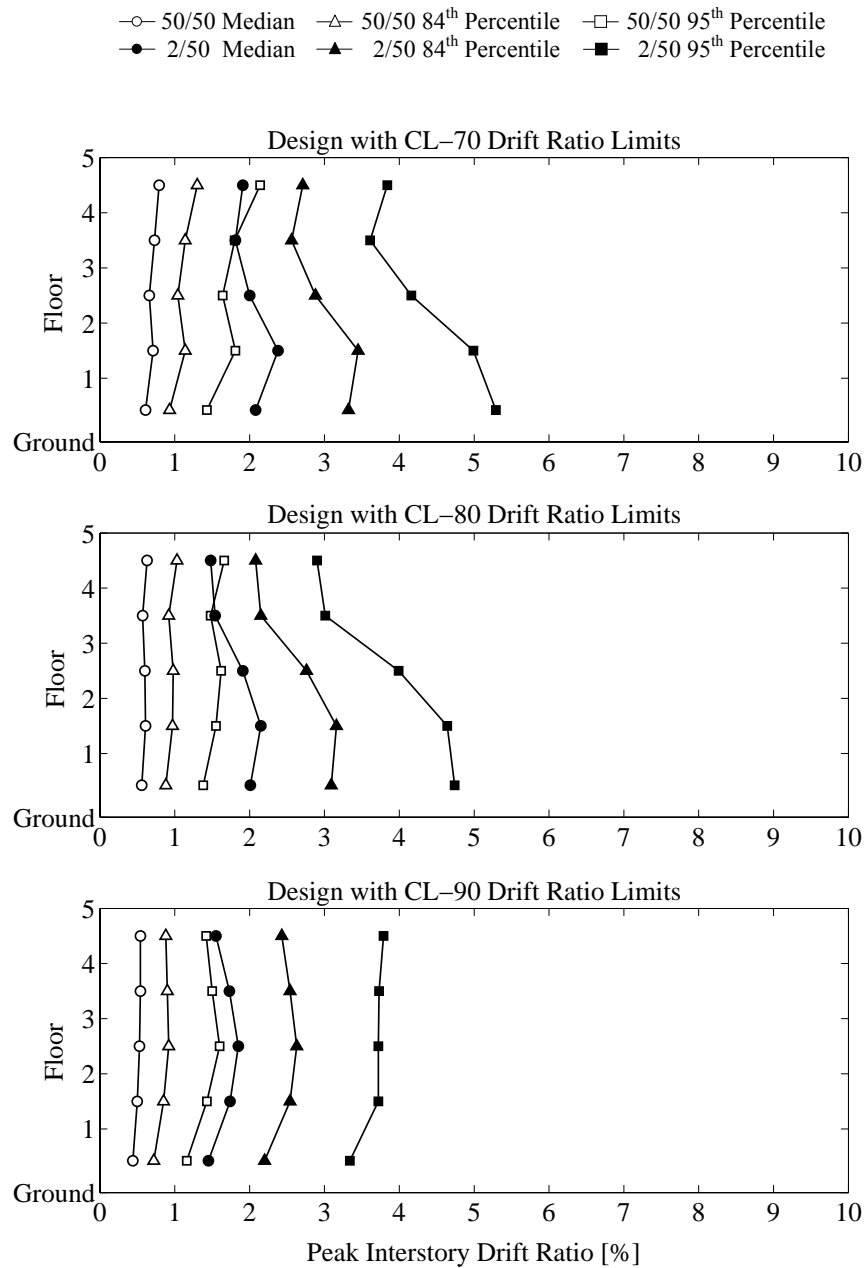


Figure 7.32 (cont'd) Peak interstory drift demand profiles at different hazard levels by time history analysis for design solutions of five section types with similar calculated damage cost obtained using varied confidence level dependent sets of drift ratio limits

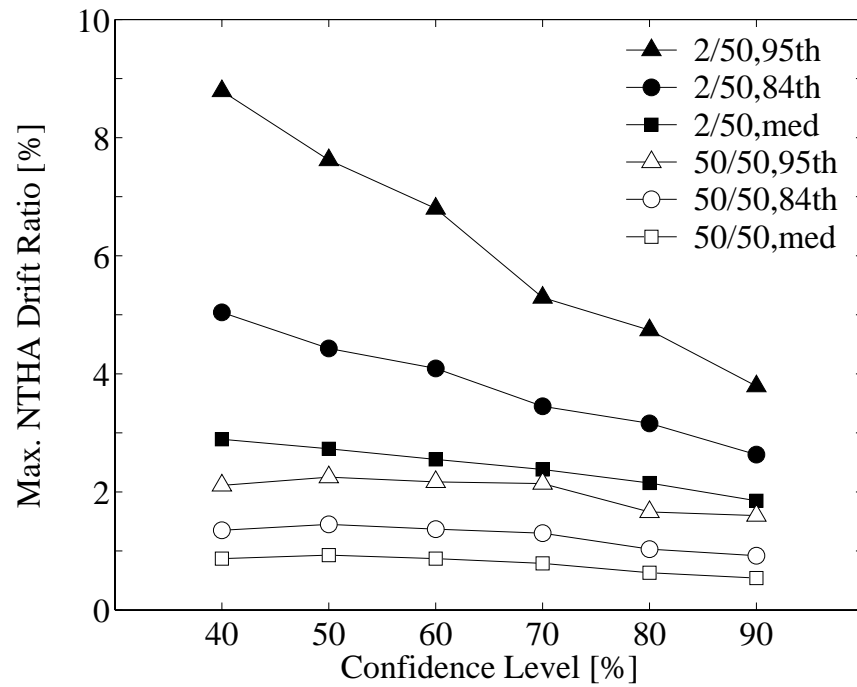


Figure 7.33 Maximum peak interstory drift demands at different hazard levels by time history analysis for design solutions of five section types with similar calculated damage cost obtained using varied confidence level dependent sets of drift ratio limits

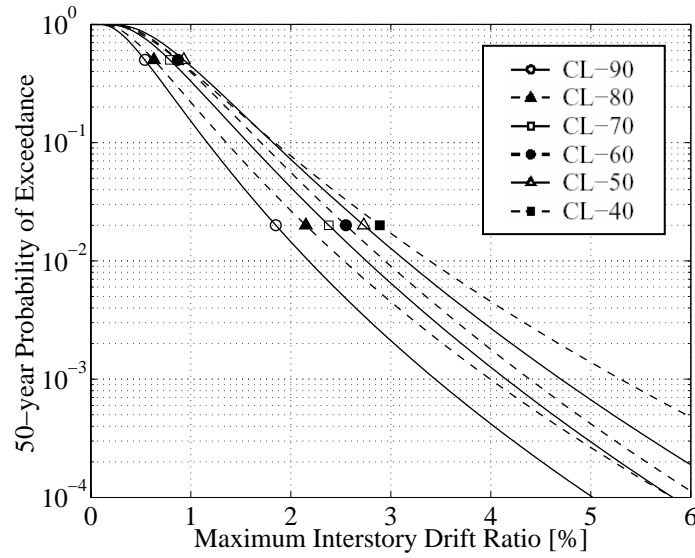


Figure 7.34 Median 50-year probabilistic performance curves by time history analysis for design solutions of five section types with similar calculated damage cost obtained using varied confidence level dependent sets of drift ratio limits

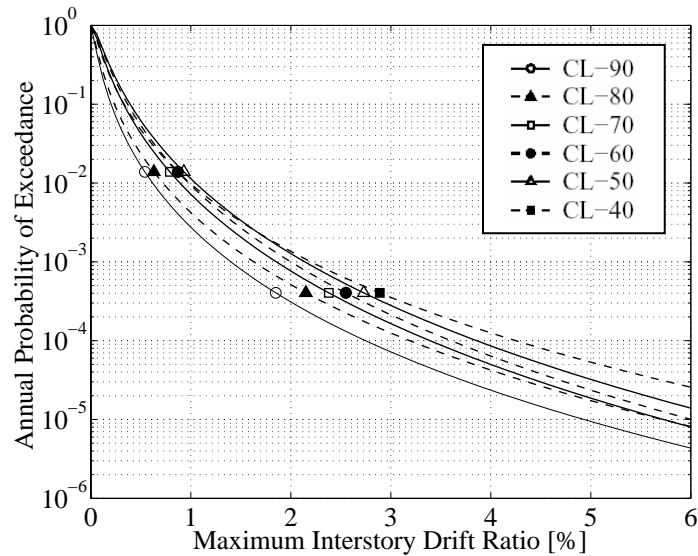


Figure 7.35 Median annual probabilistic performance curves by time history analysis for design solutions of five section types with similar calculated damage cost obtained using varied confidence level dependent sets of drift ratio limits